CHEMISTRY
A EUROPEAN JOURNAL

DOI: 10.1002/chem.200901640

Metallomacrocycles with a Difference: Macrocyclic Complexes with Exocyclic Ruthenium(II)-Containing Domains

Edwin C. Constable,* Catherine E. Housecroft,* Markus Neuburger, Pirmin J. Rösel, Silvia Schaffner, and Jennifer A. Zampese[a]

Abstract: The templated synthesis of organic macrocycles containing rings of up to 96 atoms and three 2,2′-bipyridine (bpy) units is described. Starting with the bpy-centred ligands 5,5′-bis[3-(1,4-dioxahept-6-enylphenyl)]-2,2′-bipyridine and 5,5′-bis[3-(1,4,7-trioxadec-9-enylphenyl)]-2,2′-bipyridine, we have applied Grubbs' methodology to couple the terminal alkene units of the coordinated ligands in $[FeL_3]^{2+}$ complexes. Hydrogenation and demetallation of the iron(II)-containing macrocyclic complexes results in the isolation of large organic macrocycles. The latter bind $\{Ru(bpy)_2\}$ units to give macrocyclic complexes with exocyclic ruthenium(II)-containing domains. The complex $[Ru(bpy)_2(L)]^{2+}$ (isolated as the hexafluorophosphate salt), in which L = 5,5′-bis[3-(1,4,7,10-tetraoxatridec-12-enylphenyl)]-2,2′-bipyridine, undergoes intramolecular ring-closing metathesis to yield a macrocycle which retains the exocyclic $\{Ru(bpy)_2\}$ unit. The poly(ethyleneoxy) domains in the latter macrocycle readily scavenge sodium ions, as proven by single-crystal X-ray diffraction and atomic absorption spectroscopy data for the bulk sample. In addition to the new compounds, a series of model complexes have been fully characterized, and representative single-crystal X-ray structural data are presented for iron(II) and ruthenium(II) acyclic and macrocyclic species.

Keywords: chirality · heterocycles · macrocycles · ruthenium · supramolecular chemistry

Introduction

In the first decade of the 21st century, macrocyclic chemistry can be considered a mature science.[1–4] However, the bulk of synthetic systems that have been designed for metal-ion binding are optimized for endocyclic bonding modes in which the metal ion is coordinated within the cavity of the macrocycle. In the case of macrocyclic ligands with soft donor atoms such as sulfur, selection between endocyclic and exocyclic bonding modes has been controlled by anions.[5] An alternative method for enforcing an exocyclic bonding mode is by the use of a kinetically inert centre in which a certain number of coordination sites are occupied by chelating ligands. With the aim of developing general routes for the preparation of mono- and polynuclear exocyclic complexes, we have investigated the synthesis of large-ring macrocycles containing one or more 2,2′-bipyridine (bpy) metal-binding domains.

The assembly of topologically complex architectures has become a realistic target for synthetic chemists.[6–10] For the synthesis of large macrocycles,[11] Grubbs'-catalysed ring-closing metathesis (RCM) has proved to be a very efficient strategy and operates under very mild reaction conditions.[12,13] An elegant synthetic route devised by Sauvage first introduced the concept of using a tetrahedral $\{Cu(bpy)_2\}^+$ domain coupled with Grubbs' RCM to template the formation of a catenane.[14–16] Since this breakthrough, metal-ion-templated syntheses have been applied to control a variety of ring-closing steps, thus allowing the assembly of catenanes, knots and rotaxanes.[17] Several recent examples have focused on the formation of large organic macrocycles,[18–21] and, notably, Sauvage has made use of octahedral ruthenium(II) as the templating metal centre.[22–25] In 1973, Sokolov suggested the use of an octahedral tris(chelate) template for the assembly of a trefoil knot.[26] The Grubbs' methodology provides an ideal opportunity for exploring this approach, starting with terminally

[a] Prof. Dr. E. C. Constable, Prof. Dr. C. E. Housecroft, M. Neuburger, Dr. P. J. Rösel, Dr. S. Schaffner, Dr. J. A. Zampese
Department of Chemistry
University of Basel
Spitalstrasse 51, 4056 Basel (Switzerland)
Fax: (+41) 61-267-1018
E-mail: catherine.housecroft@unibas.ch

Supporting information for this article is available on the WWW under http://dx.doi.org/10.1002/chem.200901640. It contains details of AAS determination of sodium content in $[Ru(bpy)_2(\mathbf{7})][PF_6]_2 \cdot x\mathrm{Na}[PF_6]$; hydrogen-bond contacts; and TRISPHAT experiments.

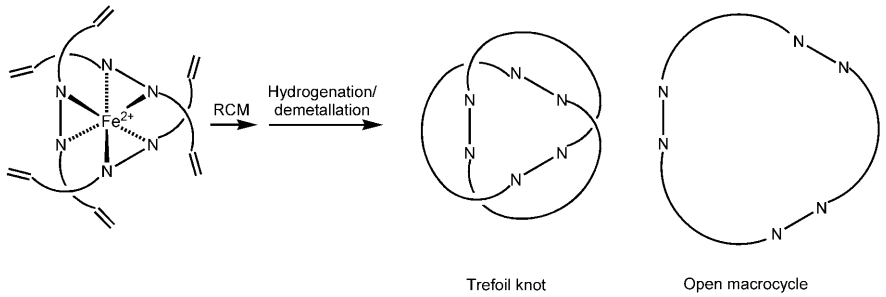

Scheme 1. Schematic representation of the synthesis of a trefoil knot or macrocycle templated by an octahedral $\{Fe(bpy)_3\}^{2+}$ unit.

alkene-functionalized bpy ligands and an $\{Fe(bpy)_3\}^{2+}$ template. Under high dilution conditions, RCM should predominate over alkene metathesis between complex cations. By optimizing the length of the spacers between the bpy domain and the alkene functionalities, in theory a threefold RCM should lead to either a trefoil knot or an open macrocycle (Scheme 1). In the event, the non-knotted topological isomers were obtained, and we report here the templated synthesis of macrocycles containing rings with up to 96 atoms and their reactions with *cis*-$[Ru(bpy)_2Cl_2]$ to form macrocyclic complexes with exocyclic coordination domains.

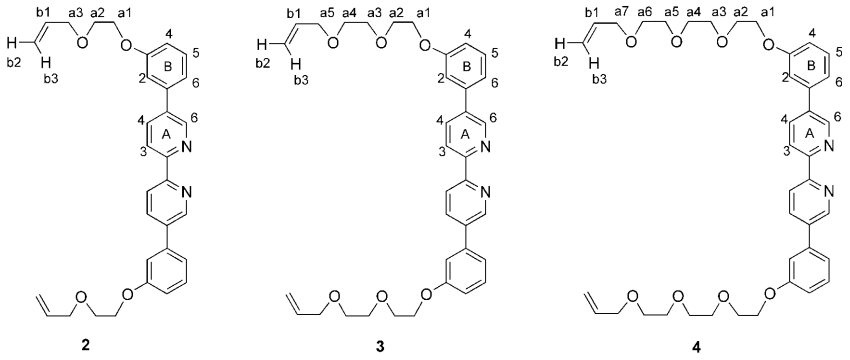

Results and Discussion

Ligand synthesis and characterization: We have previously described the synthesis of ligand **1** (structures show the

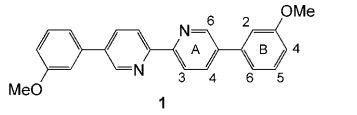

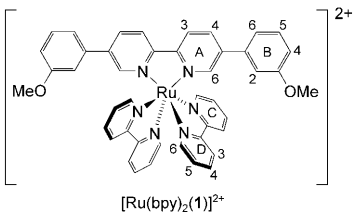

numbering and ring labelling scheme used for NMR spectroscopic assignments) and its deprotection to give 5,5′-bis(3′-hydroxyphenyl)-2,2′-bipyridine.[27] We have also reported the preparation of ligand **2** through caesium-directed Williamson's methodology by reacting 5,5′-bis(3′-hydroxyphenyl)-2,2′-bipyridine with 3-(2-bromoethoxy)prop-1-ene in the presence of Cs_2CO_3 in DMF.[28] Ligands **3** and **4**, congeners of **2** with additional ethoxy spacers, were prepared in an analogous manner to **2**. Both ligands were obtained in high yield. The highest mass (and base) peaks in the electron impact (EI) mass spectra of **3** and **4** appeared at *m*/*z* 596.3 and 685.4, respectively, and each was assigned to the parent ion. The ^1H and ^{13}C NMR spectra were fully assigned by COSY, NOESY, HMQC and HMBC techniques and were consistent with the symmetrical structures shown. The aromatic regions of the ^1H NMR spectra of CD_2Cl_2 solutions of **3** and **4** are virtually superimposable, as are the spectroscopic signatures for the alkene protons (H^{b1}, H^{b2} and H^{b3}). The aliphatic regions in the ^1H NMR spectra of the two ligands are extremely similar, with the exception of additional signals for the extra methylene groups. For both ligands, the resonances for protons H^{a1} appear as the highest-frequency aliphatic signals, with the resonances for the alkene-attached CH_2 group (H^{a5} for **3**, H^{a7} for **4**) being at the next highest frequency. The CD_2Cl_2 solution ^{13}C NMR spectra of **3** and **4** are also similar, the aromatic and alkene regions being almost superimposable, and the aliphatic regions differing only in the appearance of the additional CH_2 ^{13}C signals on going from **3** to **4**.

Model complexes: Before proceeding to the formation of macrocyclic ligands and their complexes, we describe the synthesis and characterization of the model complexes $[Fe(\mathbf{1})_3][PF_6]_2$, $[Ru(bpy)_2(\mathbf{1})][PF_6]_2$, $[Ru(bpy)_2(\mathbf{3})][PF_6]_2$ and $[Ru(bpy)_2(\mathbf{4})][PF_6]_2$. A spectroscopic and structural databank for these systems proves helpful for the assignment of spectra of the more complicated species encountered later in the discussion. The reaction between ligand **1** and $FeCl_2{\cdot}4H_2O$ in CH_2Cl_2/MeCN, followed by anion exchange and workup, led to the isolation of $[Fe(\mathbf{1})_3][PF_6]_2$ in moderate yield. The highest mass peak (also the base peak) at *m*/*z*

580.5 in the electrospray ionization (ESI) mass spectrum was assigned to $[M-2PF_6]^{2+}$, and the isotope distribution matched that calculated. Each of the ^1H and ^{13}C NMR spectra was consistent with the formation of $[Fe(\mathbf{1})_3]^{2+}$ in which each ligand is in a symmetrical environment. Compared to the signals for the free ligand **1**,[27] that assigned to proton H^{A6} is the most significantly affected by coordination, shifting from $\delta = 8.94$ ppm (**1** in $CDCl_3$) to $\delta = 7.52$ ppm (complex in CD_3CN). This is a characteristic indication that an {M(bpy)$_3$} motif has been formed and occurs because of the shielding experienced when H^{A6} lies over the π cloud of one ring of an adjacent bpy ligand. Single crystals of $[Fe(\mathbf{1})_3][PF_6]_2 \cdot 3C_2H_4Cl_2$ suitable for X-ray diffraction study were grown by layering diethyl ether over a 1,2-dichloroethane solution of the complex. Figure 1 shows the structure of the

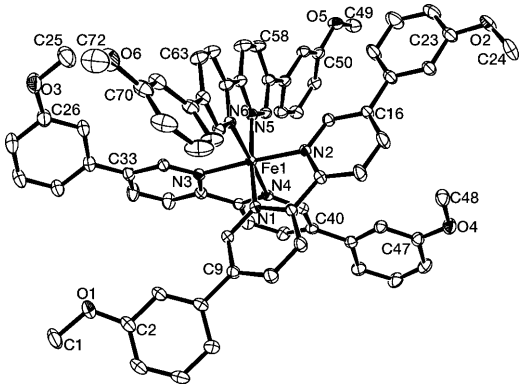

Figure 1. Molecular structure of the $[Fe(\mathbf{1})_3]^{2+}$ cation in $[Fe(\mathbf{1})_3][PF_6]_2 \cdot 3C_2H_4Cl_2$ with ellipsoids plotted at the 30% probability level; hydrogen atoms are omitted. Selected bond lengths [Å] and angles [°]: Fe1–N1 1.962(2), Fe1–N2 1.963(2), Fe1–N3 1.967(2), Fe1–N4 1.953(2), Fe1–N5 1.974(2), Fe1–N6 1.961(2); N1-Fe1-N2 81.6(1), N3-Fe1-N4 81.5(1), N5-Fe1-N6 82.3(1), N2-Fe1-N3 176.8(1), N1-Fe1-N5 173.7(1), N4-Fe1-N6 173.9(1).

$[Fe(\mathbf{1})_3]^{2+}$ cation. The compound crystallizes in the non-chiral space group *Pcab*, and so both enantiomers of the cation are present. Each ligand is significantly twisted, with the angles between the least-squares planes of adjacent rings being 33.7(2), 2.5(2) and 3.6(2)° for the ligand containing atoms N1 and N2, 34.7(2), 10.7(2) and 16.7(2)° for that with atoms N3 and N4, and 29.8(2), 6.7(2) and 29.3(2)° for the ligand containing N5 and N6. The orientations of the methoxy groups deserve comment. In the ligand containing atoms O1 and O2, the methoxy substituents are in a *transoid* arrangement, whereas in that containing O3 and O4, the two substituents both point towards the iron atom. In the third ligand, both methoxy groups (O5 and O6) are directed away from the coordination centre. These variations are most probably a result of non-classical O···H–C hydrogen bonds (see Supporting Information). Most importantly, the structural determination confirmed that the {Fe(**1**)$_3$} building block can assemble with the peripheral methoxyphenyl units and has significant flexibility by virtue of twisting about the $C_{pyridine}$–C_{phenyl} bonds.

The complex $[Ru(bpy)_2(\mathbf{1})][PF_6]_2$ was isolated in near quantitative yield by the reaction of *cis*-$[Ru(bpy)_2Cl_2]$ with ligand **1** under microwave conditions followed by anion exchange. The ESI mass spectrum exhibits peak envelopes with characteristic ruthenium isotope distributions at *m*/*z* 927.1 and 391.2, assigned to $[M-PF_6]^+$ and $[M-2PF_6]^+$, respectively. Figure 2 shows the aromatic region of the

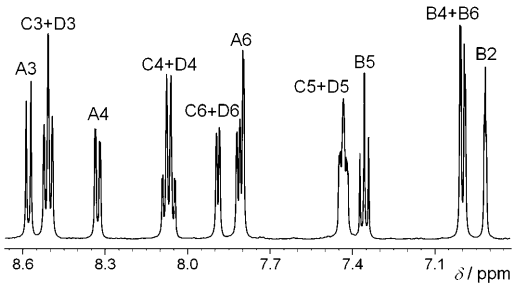

Figure 2. 500 MHz ^1H NMR spectrum of a CD_3CN solution of $[Ru(bpy)_2(\mathbf{1})][PF_6]_2$ at room temperature. See structure for atom labelling.

^1H NMR spectrum of the complex. Coordination of ligand **1** to the {Ru(bpy)$_2$} unit is accompanied in the ^1H NMR spectrum by the diagnostic shift of the signal for proton H^{A6} (from $\delta = 8.94$[27] to 7.80 ppm, **1** being in $CDCl_3$ and the complex in CD_3CN). In $[Ru(bpy)_3]^{2+}$, all 6- and 6′-protons are chemically equivalent because each lies over a chemically equivalent pyridine ring. However, in $[Ru(bpy)_2(\mathbf{1})]^{2+}$, although the pyridine rings in ligand **1** are chemically equivalent, those in each bpy ligand are chemically inequivalent. Proton H^{D6} points towards the π cloud of ring A, whereas H^{C6} lies over the second ring C. Figure 2 illustrates the observation of two signals for H^{C6} and H^{D6}, but we were unable to unambiguously assign the signals to one or other of these protons.

The anion TRISPHAT[29,30] (tris(tetrachlorobenzenediolato)phosphate(V)) is a general NMR chiral resolving reagent for chiral cationic species. Compared to the spectrum for the $[PF_6]^-$ salt, the ^1H NMR spectrum of Δ-TRISPHAT salt shows two sets of signals in roughly equal intensities arising from the diastereoisomers [Δ-Ru(bpy)$_2$(**1**)][Δ-TRISPHAT] and [Λ-Ru(bpy)$_2$(**1**)][Δ-TRISPHAT] (see Supporting Information).

X-ray-quality crystals of $[Ru(bpy)_2(\mathbf{1})][PF_6]_2 \cdot MeCN$ were grown by layering Et_2O over an MeCN solution of the complex. The structure of the cation is shown in Figure 3. The two bpy ligands deviate slightly from planarity (the angles between the least-squares planes of the rings containing N51 and N61, and N71 and N81 are 2.8(2) and 9.8(2)°), and ligand **1** is significantly twisted (the angles between the planes of the four rings are 42.3(2), 7.9(2) and 34.1(2)°). Both methoxy substituents point away from the ruthenium(II) centre, and one is involved in non-classical hydrogen bonding to aromatic CH units of adjacent cations (see Supporting Information).

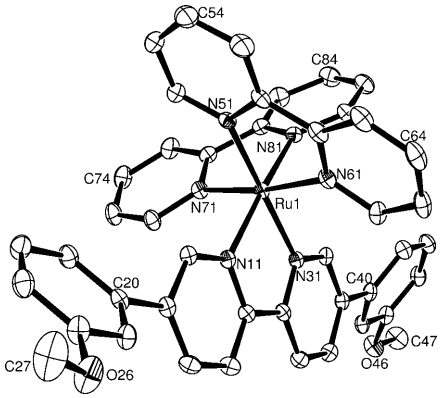

Figure 3. Molecular structure of the $[Ru(bpy)_2(\mathbf{1})]^{2+}$ cation in $[Ru(bpy)_2(\mathbf{1})][PF_6]_2 \cdot MeCN$ with ellipsoids plotted at the 30% probability level; hydrogen atoms omitted. Selected bond lengths [Å] and angles [°]: Ru1–N31 2.052(3), Ru1–N71 2.055(3), Ru1–N51 2.056(3), Ru1–N81 2.060(3), Ru1–N11 2.063(3), Ru1–N61 2.070(3); N31-Ru1-N11 78.7(1), N51-Ru1-N61 78.30(1), N71-Ru1-N81 78.9 (1), N31-Ru1-N51 175.0(1), N81-Ru1-N11 171.4(1), N71-Ru1-N61 172.4(1).

Ligands **3** and **4** react with *cis*-$[Ru(bpy)_2Cl_2]$ under microwave conditions and, following anion exchange and chromatographic workup, $[Ru(bpy)_2(\mathbf{3})][PF_6]_2$ and $[Ru(bpy)_2(\mathbf{4})][PF_6]_2$ were isolated in $\geq 90\%$ yield. The ESI mass spectrum of each complex showed molecular ions assigned to $[M-PF_6]^+$ and $[M-2PF_6]^{2+}$, each peak envelope having the expected isotope distributions. The ^1H and ^{13}C NMR spectra of the products were assigned by 2D techniques. In the ^1H NMR spectra, the shift of the signal for proton H^{A6} from $\delta = 8.93$ ppm in **3** to $\delta = 7.81$ ppm in $[Ru(bpy)_2(\mathbf{3})][PF_6]_2$, and from $\delta = 8.94$ ppm in **4** to $\delta = 7.65$ ppm in $[Ru(bpy)_2(\mathbf{4})][PF_6]_2$, was consistent with coordination of the ligands to the metal ion. The appearance of two sets of signals for the bpy ligand protons for each complex mimicked the scenario for $[Ru(bpy)_2(\mathbf{1})][PF_6]_2$ described above. The aliphatic region of the ^1H NMR spectrum of $[Ru(bpy)_2(\mathbf{3})][PF_6]_2$ was very similar to that in the free ligand **3**, which indicated that coordination of the bpy domain of **3** has little effect on the methylene and alkene protons. This was also true on going from free ligand **4** to $[Ru(bpy)_2(\mathbf{4})][PF_6]_2$.

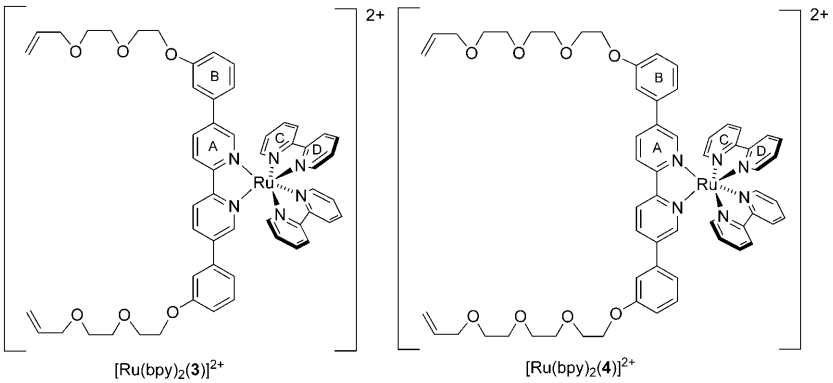

$[Ru(bpy)_2(\mathbf{3})]^{2+}$ $[Ru(bpy)_2(\mathbf{4})]^{2+}$

With the spectroscopic signatures and structural properties of the model complexes established, we were in a position to turn our attention to the use of ligands **2**–**4** and the synthesis of large macrocyclic ligands containing bpy metal-binding domains.

Templated synthesis of macrocyclic ligands: Our strategy for the formation of macrocyclic ligands containing three bpy metal-binding domains was to first prepare the iron(II) complexes $[Fe(\mathbf{2})_3]^{2+}$, $[Fe(\mathbf{3})_3]^{2+}$ and $[Fe(\mathbf{4})_3]^{2+}$, apply Grubbs' methodology to couple the terminal alkene functionalities of the coordinated ligands, and then carry out hydrogenation and demetallation. The iron(II) complexes were prepared by treating $Fe(BF_4)_2 \cdot 6H_2O$ with the respective ligand in MeCN at reflux for 3–4 days. $[Fe(\mathbf{2})_3][BF_4]_2$ and $[Fe(\mathbf{3})_3][BF_4]_2$ were isolated in near quantitative yields. The highest mass peak in the ESI mass spectrum of each complex corresponded to the $[M-2BF_4]^{2+}$ ion. The ^1H and ^{13}C NMR spectra of the two complexes confirmed the presence of one, symmetrical ligand environment in each case. The diagnostic shift in the signal for protons H^{A6} from $\delta = 8.97$ ppm in **2** to $\delta = 7.54$ ppm in $[Fe(\mathbf{2})_3]^{2+}$, and from $\delta = 8.93$ ppm in **2** to $\delta = 7.75$ ppm in $[Fe(\mathbf{3})_3]^{2+}$, confirmed the formation of $\{Fe(bpy)_3\}^{2+}$ units. Although the NMR spectroscopic data were consistent with the formation of $[Fe(\mathbf{4})_3]^{2+}$ in the reaction of $Fe(BF_4)_2 \cdot 6H_2O$ with ligand **4**, an analytically pure sample of $[Fe(\mathbf{4})_3][BF_4]_2$ could not be obtained, and we therefore focused our attention on the reactivities of $[Fe(\mathbf{2})_3]^{2+}$ and $[Fe(\mathbf{3})_3]^{2+}$.

Scheme 2 summarizes the approach taken to the formation of a macrocyclic ligand beginning with the complex $[Fe(\mathbf{2})_3]^{2+}$. A dichloromethane solution of $[Fe(\mathbf{2})_3][BF_4]_2$ was stirred at room temperature in the presence of Hoyveda–Grubbs catalyst. The progress of the reaction was monitored by ^1H NMR spectroscopy and ESI mass spectrometry. The ^1H NMR spectrum showed the disappearance of the terminal alkene protons at $\delta = 5.18$, 5.28 and 5.90 ppm, and the appearance of new signals at $\delta = 5.93$ and 5.74 ppm for the newly formed HC=CH unit (*Z* and *E* isomers). After 40 days, $>95\%$ alkene metathesis had been achieved. The crude product was demetallated by treating it with Na_2H_2EDTA (EDTA: ethylenediaminetetraacetate) in the presence of Na_2CO_3, the removal of Fe^{II} being monitored by loss of the red colour typical of the $\{Fe(bpy)_3\}$ chromophore. (Attempts to demetallate the complex with cyanide, or mixtures of H_2O_2 and NaOH, resulted in decomposition of the RCM product.) After the organic product had been extract-

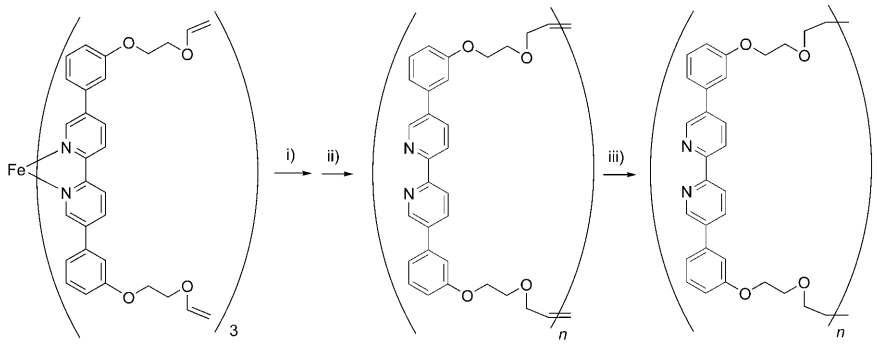

Scheme 2. Schematic representation of the methodology used to prepare a macrocyclic ligand starting with $[Fe(\mathbf{2})_3]^{2+}$: i) Hoyveda–Grubbs catalyst, CH_2Cl_2, 40 days, room temperature; ii) Na_2H_2EDTA, Na_2CO_3; iii) H_2 (1 bar), Pd/C, CH_2Cl_2/EtOH. See text for *n*.

ed, it was hydrogenated (1 bar H_2, Pd/C). Chromatographic purification of the product proved difficult, but after a combination of column and preparative thin-layer chromatographies (see Experimental Section) macrocycle **5** was obtained. The ^{1}H NMR spectrum of the product indicated that it was approximately 80% pure. In the ^{1}H NMR spectrum, the appearance of a multiplet at $\delta = 1.68$ ppm was consistent with the presence of a methylene group not directly bonded to an oxygen atom. This, along with the loss of signals in the alkene region of the spectrum, supported the formation of the final product shown in Scheme 2. The signals in the aromatic region of the spectrum were similar to those for ligand **2**, but each was shifted to a lower frequency by between 0.06 and 0.12 ppm. The highest mass and base peak in the ESI mass spectrum of the product was observed at *m*/*z* 988.0 and corresponded to $[M+Na]^+$ for a macrocycle with $n = 2$ in Scheme 2. Thus, although molecular modelling[31] had indicated that the poly(ethyleneoxy) spacers were long enough to allow coupling of all three ligands in $[Fe(\mathbf{2})_3]^{2+}$, in practice macrocycle **5** ($n = 2$ in Scheme 2) was formed by the coupling of only two coordinated ligands. This was confirmed from the structural characterization of the product of the reaction of ligand **5** with *cis*-$[Ru(bpy)_2Cl_2]$ described later.

The ring-closing strategy described above was also applied to $[Fe(\mathbf{3})_3]^{2+}$. However, in this case, it was more efficient to carry out the hydrogenation step before demetallation. Careful chromatographic purification of the product resulted in the isolation of analytically pure macrocycle **6** in 26% yield. A base peak at *m*/*z* 1734.6 in the ESI mass spectrum confirmed the formulation of **6**, the peak being assigned to $[M+Na]^+$. The ^{1}H and ^{13}C NMR spectra of **6** were consistent with the symmetrical structure shown. The aromatic region of the ^{1}H NMR spectrum appeared very similar to that of ligand **3**, with signals shifted only 0.02 to 0.05 ppm to lower frequency on going from **3** to **6**. That complete hydrogenation had been achieved was supported by the disappearance of signals in the alkene region and the appearance of a multiplet at $\delta = 1.62$ ppm assigned to H^{a6}.

Ruthenium(II) complexes of ligands 5 and 6: Ligand **5** was treated with two molar equivalents of *cis*-$[Ru(bpy)_2Cl_2]$ in ethanol under microwave conditions. After anion exchange and chromatographic workup, orange $[\{Ru(bpy)_2\}_2(\mathbf{5})][PF_6]_4$ was isolated in 46% yield. The solution ^{1}H NMR spectrum of the product indicated a symmetrical structure, and revealed one set of signals for the bpy unit of ligand **5** and two sets of signals for the protons of each bpy ligand. By analogy with the discussion for $[Ru(bpy)_2(\mathbf{1})][PF_6]_2$ above (see Figure 2), the data were consistent with the structure shown. The dominant peak envelopes in the ESI mass spectrum of the complex appeared at *m*/*z* 1041.3, 646.0 and 448.2 and were assigned to $[M-2PF_6]^{2+}$, $[M-3PF_6]^{3+}$ and $[M-4PF_6]^{4+}$, respectively. The isotope distribution of each envelope matched that simulated.

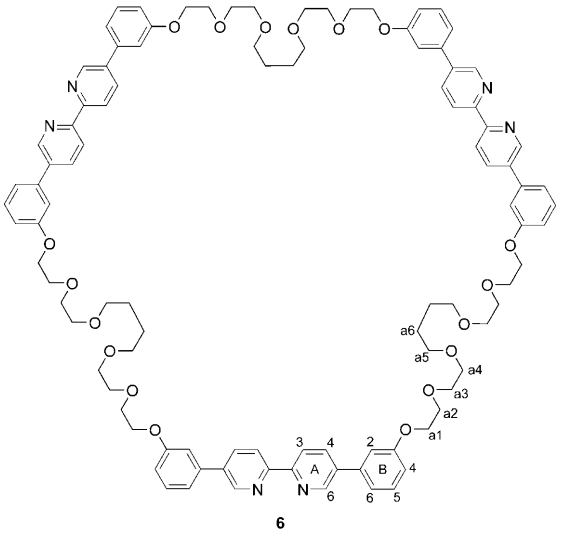

Single crystals of $[\{Ru(bpy)_2\}_2(\mathbf{5})][PF_6]_4 \cdot C_2H_4Cl_2 \cdot 2.5EtOAc$ were grown by layering ethyl acetate over a 1,2-dichloroethane solution of $[\{Ru(bpy)_2\}_2(\mathbf{5})][PF_6]_4$. The complex crystallizes in the centrosymmetric $P\bar{1}$ space group and was obtained in the homochiral form (Figure 4) with the unit cell

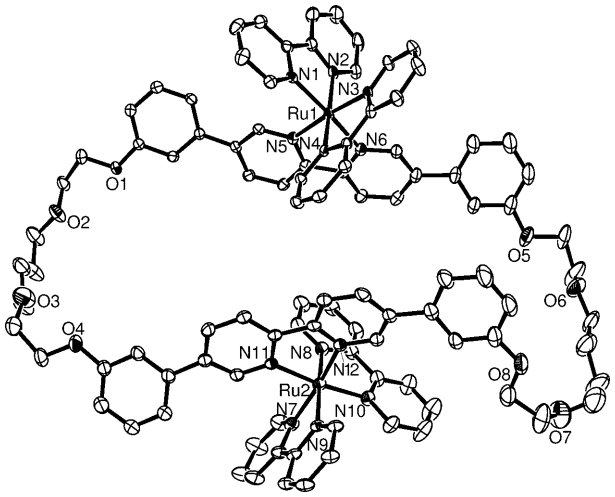

Figure 4. Molecular structure of the $[\{Ru(bpy)_2\}_2(\mathbf{5})]^{4+}$ cation in $[\{Ru(bpy)_2\}_2(\mathbf{5})][PF_6]_4 \cdot C_2H_4Cl_2 \cdot 2.5EtOAc$ with ellipsoids plotted at the 30% probability level; hydrogen atoms omitted. For each of the disordered C and O atoms in the macrocycle, one position only is shown. Selected bond lengths [Å] and angles [°]: Ru1–N1 2.052(4), Ru1–N2 2.054(3), Ru1–N3 2.060(3), Ru1–N4 2.050(3), Ru1–N5 2.047(3), Ru1–N6 2.063(4), Ru2–N7 2.056(4), Ru2–N8 2.069(4), Ru2–N9 2.074(3), Ru2–N10 2.055(4), Ru2–N11 2.057(4), Ru2–N12 2.063(4); N1-Ru1-N2 79.3(1), N3-Ru1-N4 79.2(1), N5-Ru1-N6 78.8(1), N2-Ru1-N4 171.8(2), N3-Ru1-N5 174.4(1), N1-Ru1-N6 172.3(1), N8-Ru2-N10 78.7(2), N7-Ru2-N9 79.1(2), N11-Ru2-N12 79.3(2), N8-Ru2-N9 174.1(2), N10-Ru2-N11 173.4(2), N7-Ru2-N12 168.2(2).

containing one ΔΔ and one ΛΛ isomer. Both $\{Ru(bpy)_2\}$ units are directed towards the outside of the macrocycle, and bond parameters within the coordination sphere of each ruthenium ion are unexceptional. Both poly(ethyleneoxy) chains, two $[PF_6]^-$ ions and the 1,2-dichloroethane solvent molecules suffer from disorder, and have been modelled using multiple positions and appropriate restraints. The Ru1···Ru2 separation across the macrocyclic cavity is 10.012(1) Å, and the aromatic rings are too far apart for there to be any intramolecular π stacking. The cavity of the $[\{Ru(bpy)_2\}_2(\mathbf{5})]^{4+}$ cation hosts one disordered $[PF_6]^-$ ion and one ethyl acetate solvent molecule, each sandwiched between pairs of aromatic rings (Figure 5).

Ligand **6** was treated with three molar equivalents of *cis*-$[Ru(bpy)_2Cl_2]$ in ethanol in a microwave reactor. After anion exchange, orange $[\{Ru(bpy)_2\}_3(\mathbf{6})][PF_6]_6$ was isolated in 92% yield. Analytically pure material was obtained without the need for chromatographic purification. The highest mass peak in the ESI mass spectrum was observed at *m*/*z* 1765.7 and was assigned to $[M-2PF_6]^{2+}$. A series of peak envelopes at *m*/*z* 1128.5, 811.1, 619.8 and 492.4 arose from sequential loss of $[PF_6]^-$, and all peaks exhibited the correct isotopic distributions. The number of signals in each of the

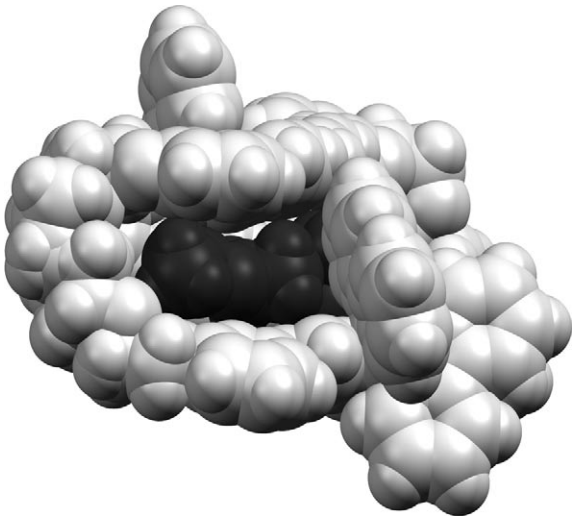

Figure 5. Space-filling representation of the $[\{Ru(bpy)_2\}_2(\mathbf{5})]^{4+}$ cation in $[\{Ru(bpy)_2\}_2(\mathbf{5})][PF_6]_4 \cdot C_2H_4Cl_2 \cdot 2.5EtOAc$ showing the ethyl acetate molecule (visible above in the front half of the cavity) and $[PF_6]^-$ ion hosted within the macrocyclic cavity.

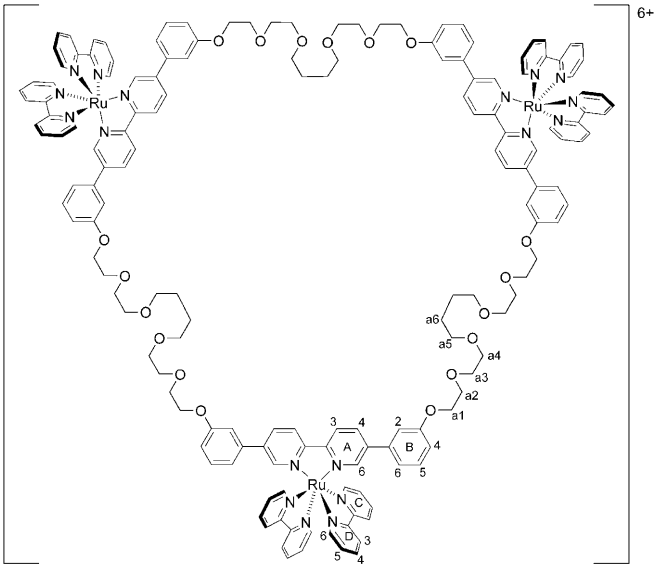

$[\{Ru(bpy)_2\}_3(\mathbf{6})]^{6+}$

^1H and ^{13}C NMR spectra was consistent with the symmetrical structure shown. The diagnostic shift of protons H^{A6} upon coordination, and the appearance of one set of signals for the bpy unit of **6** and two sets of signals for the protons of each bpy ligand, provided confirmation that each bpy domain in ligand **6** had bound a $\{Ru(bpy)_2\}$ unit. The presence of three stereogenic ruthenium(II) centres in $[\{Ru(bpy)_2\}_3(\mathbf{6})]^{6+}$ leads to the possibility of a pair of homochiral ΛΛΛ/ΔΔΔ stereoisomers and three pairs of heterochiral ΛΛΔ/ΔΔΛ stereoisomers (Figure 6). The addition of approximately six equivalents of $[Et_4N][\Delta\text{-TRISPHAT}]$ (see Supporting Information) to a CD_2Cl_2 solution of $[\{Ru(bpy)_2\}_3(\mathbf{6})][PF_6]_6$ resulted in the ^1H NMR spectrum becoming far more complex, which can be attributed to the pres-

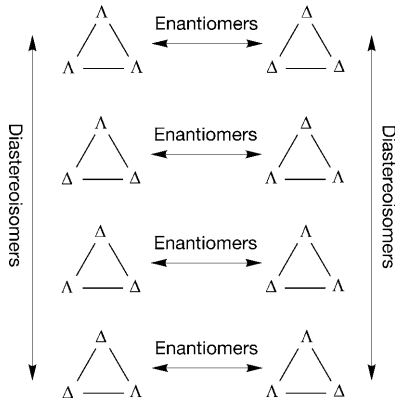

Figure 6. Schematic representation of the stereoisomers possible for [{Ru(bpy)$_2$}$_3$(**6**)]$^{6+}$.

ence of [ΔΔΔ-{Ru(bpy)$_2$}$_3$(**6**)][Δ-TRISPHAT]$_6$, [ΛΛΛ-{Ru(bpy)$_2$}$_3$(**6**)][Δ-TRISPHAT]$_6$, [ΛΛΔ-{Ru(bpy)$_2$}$_3$(**6**)][Δ-TRISPHAT]$_6$ and [ΔΔΛ-{Ru(bpy)$_2$}$_3$(**6**)][Δ-TRISPHAT]$_6$. However, we were unable to unambiguously assign the spectrum.

RCM with [Ru(bpy)$_2$(4)]$^{2+}$: Because we were unable to proceed with the use of [Fe(**4**)$_3$]$^{2+}$ for RCM, we decided instead to apply Grubbs' methodology (Scheme 2) to [Ru(bpy)$_2$(**4**)]$^{2+}$. A CH_2Cl_2 solution of [Ru(bpy)$_2$(**4**)][PF$_6$]$_2$ was treated with Hoyveda–Grubbs catalyst at room temperature and the reaction was monitored periodically with ^{1}H NMR spectroscopy and ESI mass spectrometry. After 17 days, the diagnostic ^{1}H NMR signals for the alkene protons in [Ru(bpy)$_2$(**4**)]$^{2+}$ had disappeared. Hydrogenation of the unsaturated intermediate, followed by chromatographic purification, resulted in the isolation of an orange solid. The ESI mass spectrum of the latter exhibited peaks at *m*/*z* 1217.6 and 536.2, consistent with intramolecular RCM in [Ru(bpy)$_2$(**4**)]$^{2+}$ and the formation of [Ru(bpy)$_2$(**7**)]$^{2+}$. The ^{1}H

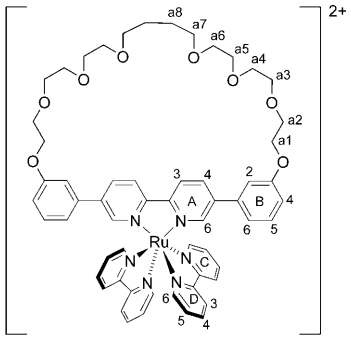

[Ru(bpy)$_2$(**7**)]$^{2+}$

and ^{13}C NMR spectra were also consistent with this formulation. The methylene protons H^{a8} gave rise to a signal at $\delta =$ 1.58 ppm, which is similar to the non-oxygen-attached CH_2 groups in the macrocycles described above. However, the signal for H^{a7} (the assignment being confirmed by a COSY cross peak to H^{a8}) was observed at $\delta = 2.30$ ppm, significantly shifted to lower frequency when compared with the signals for the other OCH_2 protons ($\delta = 3.38$ to 3.98 ppm). In the solid-state structure (see below), the poly(ethyleneoxy) chain wraps around the {Ru(bpy)$_3$} unit. Assuming that this same arrangement is maintained in solution, then the O-$(CH_2)_4$O unit lies within the cleft between the two bpy ligands, the H^{a7} protons being close to the bpy π clouds.

Elemental analytical data for the orange product did not, however, correspond to [Ru(bpy)$_2$(**7**)][PF$_6$]$_2$, but we were fortunate in being able to grow X-ray-quality crystals from an MeCN solution of the complex layered with Et_2O. The X-ray diffraction study revealed the crystalline sample to be [Ru(bpy)$_2$(**7**)][NaRu(bpy)$_2$(**7**)][PF$_6$]$_5$. The source of the sodium ions is not clear, and we can only assume that they are extracted by the macrocyclic ligand during chromatographic workup. Attempts to prepare sodium-free samples of the complex failed. The sodium content of the bulk sample was determined by atomic absorption spectroscopy (AAS; see Supporting Information) and the results indicated that (35 ± 10) % of the [Ru(bpy)$_2$(**7**)]$^{2+}$ cations contained Na$^+$. The role of the sodium ions in the complex was revealed from the results of the single-crystal X-ray diffraction study. The complex crystallizes in the $P\bar{1}$ space group and the asymmetric unit contains one [Ru(bpy)$_2$(**7**)]$^{2+}$ and one [NaRu(bpy)$_2$(**7**)]$^{3+}$ cation. Significant problems were encountered from disordered solvent molecules that fill the void space between the cations. As these solvent molecules were not important to the overall structure, they were removed by the program SQUEEZE.[32] The flexibility of the poly(ethyleneoxy) chains in both cations led to varying degrees of disorder and, understandably, some of the atom positions in the chains are poorly defined. Figure 7a shows the structure of the [Ru(bpy)$_2$(**7**)]$^{2+}$ cation. Each of the atoms in the chain from O1 to O9 is disordered and each has been modelled over two positions with fractional occupancies of 0.5/0.5. One phenyl ring is also disordered. Bond parameters within the ruthenium(II) coordination sphere are unexceptional. The {Ru(bpy)$_2$} unit is directed towards the macrocyclic cavity, with the O$(CH_2)_4$O unit residing between the two bpy ligands (Figure 7b). As in [Ru(bpy)$_2$(**7**)]$^{2+}$, the {Ru(bpy)$_2$} unit in the [NaRu(bpy)$_2$(**7**)]$^{3+}$ cation points towards the macrocyclic cavity; the sodium ion lies on the opposite side of the macrocycle. The Na$^+$ ion is coordinated by three O donor atoms (O51–Na1 2.686(4), O54–Na1 2.306(4), O57–Na1 2.619(5) Å) and by two [PF$_6$]$^-$ ions (Na1–F34 2.429(5), Na1–F32 2.473(6), Na1–F56 2.488(5), Na1–F54 2.507(7), Na1–F55 2.532(6) Å). Figure 8 shows the close C–H···F contacts between the centrosymmetric pair of [NaRu(bpy)$_2$(**7**)]$^{3+}$ cations in the unit cell. The non-sodium-bound [PF$_6$]$^-$ ions are also involved in extensive C–H···F interactions, which dominate the cation–anion packing.

Absorption, emission and electrochemical properties of the ruthenium(II) complexes: The absorption spectra of CH_2Cl_2 solutions of the model complex [Ru(bpy)$_2$(**1**)][PF$_6$]$_2$ and each of the macrocyclic complexes [Ru(bpy)$_2$(**7**)][PF$_6$]$_2$,

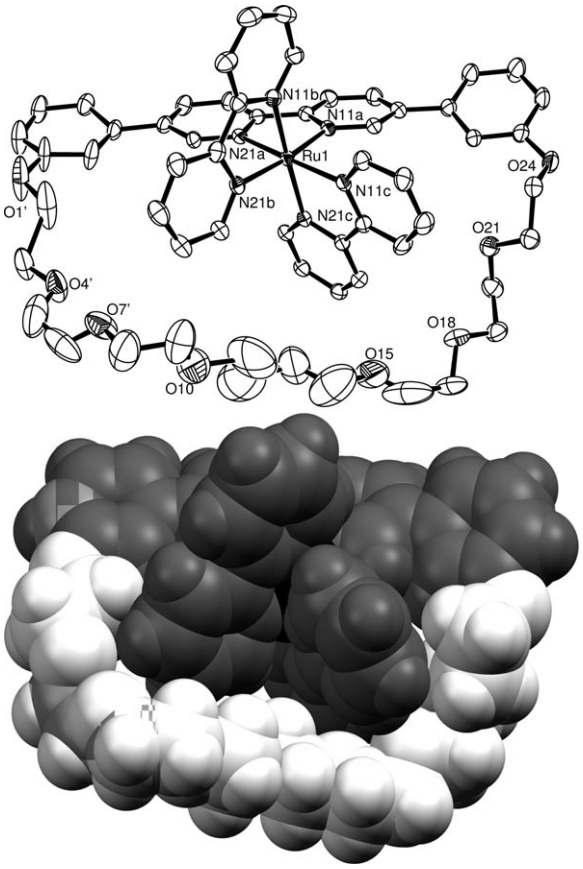

Figure 7. a) Molecular structure of the $[Ru(bpy)_2(\mathbf{7})]^{2+}$ cation in $[Ru(bpy)_2(\mathbf{7})][NaRu(bpy)_2(\mathbf{7})][PF_6]_5$; hydrogen atoms omitted. Ellipsoids are plotted at 30% probability level. For disordered atoms (see text), only one position for each atom is shown. Selected bond lengths [Å] and angles [°]: Ru1–N11a 2.058(3), Ru1–N11b 2.060(3), Ru1–N21a 2.064(3), Ru1–N21c 2.064(3), Ru1–N21b 2.067(3), Ru1–N11c 2.071(3); N11a-Ru1-N21a 78.3(1), N11b-Ru1-N21b 79.0(1), N21c-Ru1-N11c 78.9(1), N11b-Ru1-N21c 174.0(1), N11a-Ru1-N21b 173.0(1), N21a-Ru1-N11c 173.1(1). b) Space-filling diagram of the $[Ru(bpy)_2(\mathbf{7})]^{2+}$ cation (Ru, black; poly(ethyleneoxy) chain, pale grey; aromatic rings, dark grey).

$[\{Ru(bpy)_2\}_2(\mathbf{5})][PF_6]_4$ and $[\{Ru(bpy)_2\}_3(\mathbf{6})][PF_6]_6$ exhibit a metal-to-ligand charge transfer band at 457 nm in addition to a series of higher-energy intense absorptions originating from ligand-based $\pi^*\leftarrow\pi$ transitions. Excitation of each complex at around 350 nm (see Experimental Section) led to a single emission (616 nm for $[Ru(bpy)_2(\mathbf{1})]^{2+}$, 641 nm for $[Ru(bpy)_2(\mathbf{7})]^{2+}$, 617 nm for $[\{Ru(bpy)_2\}_2(\mathbf{5})]^{4+}$ and 621 nm for $[\{Ru(bpy)_2\}_3(\mathbf{6})]^{6+}$).

The electrochemical properties of the complexes were studied by cyclic and square-wave voltammetry and are summarized in Table 1. Each complex undergoes a single, reversible metal-centred oxidation at slightly higher potential than $[Ru(bpy)_3]^{2+}$ (0.89 V under the same experimental conditions as for the complexes studied here). Each complex undergoes a series of ligand-based reductions which, for the di- and trinuclear complexes, are irreversible, but tend to be reversible for the mononuclear species.

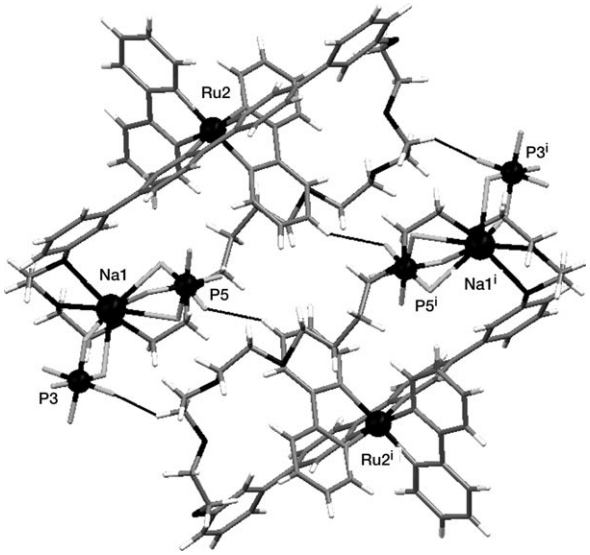

Figure 8. Centrosymmetric pair of $[NaRu(bpy)_2(\mathbf{7})]^{3+}$ cations, each associated with two $[PF_6]^-$ anions in $[Ru(bpy)_2(\mathbf{7})][NaRu(bpy)_2(\mathbf{7})][PF_6]_5$. Symmetry code $i=2-x, -y, 1-z$.

Table 1. Redox potentials for $[Ru(bpy)_2(\mathbf{1})][PF_6]_2$, $[Ru(bpy)_2(\mathbf{7})][PF_6]_2$, $[\{Ru(bpy)_2\}_2(\mathbf{5})][PF_6]_4$ and $[\{Ru(bpy)_2\}_3(\mathbf{6})][PF_6]_6$ (each in MeCN, versus ferrocene/ferrocenium).

Cation	$E(Ru^{2+}/Ru^{3+})$ [V]	Ligand-based reductions [V][a]
$[Ru(bpy)_2(\mathbf{1})]^{2+}$	0.903	−1.60, −1.87, −2.10, −2.41
$[Ru(bpy)_2(\mathbf{7})]^{2+}$	0.904	−1.60(irr), −1.92, −2.12, −2.41
$[\{Ru(bpy)_2\}_2(\mathbf{5})]^{4+}$	0.919	−1.48(irr), −1.60(irr), −1.85(irr), −2.15(irr), −2.44(irr)
$[\{Ru(bpy)_2\}_3(\mathbf{6})]^{6+}$	0.927	−1.57(irr), −1.97(irr), −2.21(irr), −2.42(irr)

[a] Reversible unless otherwise stated; irr: irreversible.

Conclusions

By using bpy-centred ligands with terminal alkene functionalities, we have illustrated the application of Grubbs' methodology to couple the alkene units of the coordinated ligands in $[FeL_3]^{2+}$ complexes (L = **2** or **3**). Hydrogenation and demetallation of the iron(II)-containing macrocyclic complexes results in the isolation of organic macrocycles containing up to 96 atoms and three bpy units. The latter bind $\{Ru(bpy)_2\}$ units to give macrocyclic complexes with exocyclic ruthenium(II)-containing domains. For ligand **4** (which contains the longest poly(ethyleneoxy) chains in our study), intramolecular RCM starting from $[Ru(bpy)_2(\mathbf{4})]^{2+}$ leads to a macrocycle which retains the exocyclic $\{Ru(bpy)_2\}$ unit. The poly(ethyleneoxy) domains in the latter macrocycle are capable of scavenging sodium ions, as proven by single-crystal X-ray diffraction and by AAS data for the bulk sample. The ligands presented herein were the result of an attempt to prepare a trefoil knot through the Sokolov approach at a single metal centre. In the event, the non-knotted topological isomers were obtained but the exquisite con-

trol over the stoichiometry of the reaction through the chain length of the spacer prompted us to study these systems in detail.

Experimental Section

General: ^{1}H and ^{13}C NMR spectra were recorded (≈295 K) on Bruker Avance DRX-600, DRX-500 and DPX-400 MHz spectrometers; chemical shifts were relative to residual solvent peaks with TMS $\delta = 0$ ppm for ^{1}H and ^{13}C, and relative to $CF(^{35}Cl)_3$ in $CDCl_3$ for ^{19}F (external reference). NMR spectra were assigned by using distortionless enhancement by polarization transfer (DEPT) and 2D techniques (COSY, NOESY, HMQC and HMBC). Infrared spectra were recorded on a Shimadzu FTIR-8400S spectrophotometer (solid samples, Golden Gate diamond attenuated total reflectance accessory). ESI mass spectra were recorded with Finnigan MAT LCQ or Bruker Esquire 3000^{plus} instruments, and EI mass spectra with a VG 70-250 instrument. Electronic absorption and emission spectra were recorded on a Varian Cary 5000 spectrophotometer and a Shimadzu RF-5301 PC spectrofluorometer, respectively. Microwave reactions were carried out in a Biotage Initiator 8 reactor. Solvents were distilled before use, and reactions were carried out under N_2. Electrochemical measurements were performed by using an Eco Chemie Autolab PGSTAT 20 apparatus with a glassy carbon working electrode, platinum mesh for counter electrode, and silver wire as reference electrode. Compounds were dissolved and measured in dry and argon-purged MeCN with 0.1 M $[n\mathrm{Bu_4N}][PF_6]$ as supporting electrolyte. The scan rate was 100 mV s^{-1} and ferrocene was added as an internal standard at the end of every experiment. AAS measurements: see the Supporting Information. *cis*-$[Ru(bpy)_2Cl_2]$,[33] 5,5′-bis(3′-hydroxyphenyl)-2,2′-bipyridine[27] and ligands **1**[27] and **2**[28] were prepared as previously reported. Second-generation Hoyveda–Grubbs catalyst and $[Et_4N][\Delta$-TRISPHAT] were purchased from Aldrich and Pd/C from Avocado, and were used as received.

$[Fe(\mathbf{1})_3][PF_6]_2$: Ligand **1** (249 mg, 676 μmol) was dissolved in CH_2Cl_2 (2 mL) and MeCN (10 mL). An aqueous solution containing an excess of $FeCl_2{\cdot}4H_2O$ (45.0 mg, 355 μmol) was added causing an immediate colour change to red. The reaction mixture was heated at reflux for 2 days, and then the organic solvents were removed in vacuo. An excess of aqueous NH_4PF_6 was added. The aqueous phase was extracted with CH_2Cl_2 (3× 50 mL) and the combined organic layers were dried over $MgSO_4$. Removal of solvent and recrystallization from CH_2Cl_2/Et_2O yielded $[Fe(\mathbf{1})_3][PF_6]_2$ (131 mg, 90 mmol, 35%). M.p. 179–182 °C; ^{1}H NMR (400 MHz, $CDCl_3$): $\delta = 8.52$ (d, $J = 8.3$ Hz, 6H; H^{A3}), 8.25 (d, $J = 8.4$ Hz, 6H; H^{A4}), 7.52 (s, 6H; H^{A6}), 7.18 (t, $J = 8.0$ Hz, 6H; H^{B5}), 6.81 (d, $J = 8.2$ Hz, 6H; H^{B6}), 6.76 (d, $J = 7.4$ Hz, 6H; H^{B4}), 6.69 (s, 6H; H^{B2}), 3.57 ppm (s, 18H; H^{Me}); ^{13}C NMR (101 MHz, $CDCl_3$): $\delta = 159.8$ (C^{B3}), 156.8 (C^{A2}), 151.3 (C^{A6}), 139.3 (C^{A5}), 136.6 (C^{A4}), 135.0 (C^{B1}), 130.2 (C^{B5}), 123.6 (C^{A3}), 118.6 (C^{B6}), 114.8 (C^{B4}), 111.8 (C^{B2}), 54.8 ppm (C^{Me}); IR (solid): $\tilde{\nu} = 2935$w, 2833w, 1717w, 1601m, 1582m, 1504m, 1470s, 1448m, 1433m, 1371m, 1304w, 1288m, 1246w, 1219m, 1173w, 1153m, 1051m, 1024m, 995m, 822s, 777m, 729m, 687w, 667m, 619m, 606m, 555m cm^{-1}; ESIMS: m/z 580.5 $[M-2PF_6]^{2+}$ (calcd 580.2); elemental analysis calcd (%) for $C_{72}H_{60}F_{12}FeN_6O_6P_2$: C 59.60, H 4.17, N 5.79; found C 59.30, H 4.36, N 5.55.

$[Ru(bpy)_2(\mathbf{1})][PF_6]_2$: 5,5′-Bis(3-methoxyphenyl)-2,2′-bipyridine (86.6 mg, 235 μmol) and *cis*-$[Ru(bpy)_2Cl_2]$ (116 mg, 240 μmol) were suspended in EtOH (5 mL). The reaction mixture was heated in a microwave reactor for 40 min at 140 °C. An excess of aqueous NH_4PF_6 (≈4 mmol, 100 mL) was added to the orange solution. An orange precipitate formed which was isolated by filtration and washed with water (50 mL) and ether (50 mL) to yield $[Ru(bpy)_2(\mathbf{1})][PF_6]_2$ (234 mg, 218 μmol, 93%) as an orange powder. M.p. 327–329 °C; ^{1}H NMR (500 MHz, CD_3CN): $\delta = 8.58$ (d, $J = 8.5$ Hz, 2H; H^{A3}), 8.51 (m, 4H; H^{C3+D3}), 8.33 (dd, $J = 2.0$, 8.5 Hz, 2H; H^{A4}), 8.07 (td, $J = 1.3$, 8.0 Hz, 4H; H^{C4+D4}), 7.89 (d, $J = 5.3$ Hz, 2H; $H^{C6/D6}$), 7.82 (d, $J = 5.3$ Hz, 2H; $H^{D6/C6}$), 7.80 (d, $J = 1.8$ Hz, 2H; H^{A6}), 7.44 (m, 4H; H^{C5+D5}), 7.36 (t, $J = 8.0$ Hz, 2H; H^{B5}), 7.00 (dd, $J = 2.0$, 8.0 Hz, 4H; H^{B4+B6}), 6.92 (t, $J = 2.0$ Hz, 2H; H^{B2}), 3.77 ppm (s, 6H; H^{Me}); ^{13}C NMR (126 MHz, CD_3CN) $\delta = 161.4$ (C^{B3}), 158.3 (C^{D2}), 158.0 (C^{C2}), 156.5 (C^{A2}), 153.1 (C^{A6}), 150.0 (C^{C6+D6}), 140.6 (C^{B1}), 138.9 ($C^{C4/D4}$), 138.85 ($C^{C4/D4}$), 137.2 (C^{A5}), 136.8 (C^{A4}), 131.6 (C^{B5}), 128.7 (C^{C5}), 128.6 (C^{D5}), 125.5 ($C^{A3/C3/D3}$), 125.33 ($C^{A3/C3/D3}$), 125.32 ($C^{A3/C3/D3}$), 120.4 ($C^{B4/B6}$), 116.3 ($C^{B4/B6}$), 113.3 (C^{B2}), 56.2 ppm (OMe); ^{19}F NMR (376 MHz, CD_3CN) $\delta = -74.1$ ppm (d, $J = 706$ Hz); IR (solid): $\tilde{\nu} = 3088$w, 2934w, 1601w, 1578w, 1464m, 1447m, 1427m, 1285w, 1215w, 1171w, 1051w, 1028w, 878w, 829s, 791m, 762m, 731m, 698w cm^{-1}; UV/Vis (CH_2Cl_2): λ_{max} (ε) = 457 (15000), 318 sh (46500), 289 nm (85900 mol^{-1} dm^3 cm^{-1}); emission (CH_2Cl_2, $\lambda_{exc} = 350$ nm): $\lambda_{max} = 616$ nm; ESIMS: m/z 391.2 $[M-2PF_6]^{2+}$ (calcd 391.1), 927.1 $[M-PF_6]^+$ (calcd 927.2); elemental analysis calcd (%) for $C_{44}H_{36}F_{12}N_6O_2P_2Ru$: C 49.31, H 3.39, N 7.86; found C 49.20, H 3.39, N 7.70.

5,5′-Bis[3-(1,4,7-trioxadec-9-enylphenyl)]-2,2′-bipyridine (3): 5,5′-Bis(3′-hydroxyphenyl)-2,2′-bipyridine (2.40 g, 7.05 mmol), 1-bromo-3,6-dioxanon-8-ene (3.24 g, 15.5 mmol) and Cs_2CO_3 (8.00 g, 24.5 mmol) were dissolved in dry DMF (200 mL). The reaction mixture was heated for 4 days at 120 °C. Removal of DMF, column chromatography (SiO_2, CH_2Cl_2/MeOH 49:1) and filtration over Al_2O_3 yielded **3** as a colourless crystalline solid (3.33 g, 5.58 mmol, 79%). M.p. 73–75 °C; ^{1}H NMR (500 MHz, CD_2Cl_2): $\delta = 8.93$ (s, 2H; H^{A6}), 8.55 (d, $J = 8.2$ Hz, 2H; H^{A3}), 8.06 (dd, $J = 2.2$, 8.3 Hz, 2H; H^{A4}), 7.43 (t, $J = 7.9$ Hz, 2H; H^{B5}), 7.29 (d, $J = 7.7$ Hz, 2H; H^{B6}), 7.24 (m, 2H; H^{B2}), 6.99 (dd, $J = 2.1$, 8.2 Hz, 2H; H^{B4}), 5.92 (m, 2H; H^{b1}), 5.27 (dd, $J = 1.6$, 17.2 Hz, 2H; H^{b3}), 5.16 (dd, $J = 1.5$, 10.4 Hz, 2H; H^{b2}), 4.21 (m, 4H; H^{a1}), 4.01 (m, 4H; H^{a5}), 3.88 (m, 4H; H^{a2}), 3.71 (m, 4H; H^{a3}), 3.62 ppm (m, 4H; H^{a4}); ^{13}C NMR (126 MHz, CD_2Cl_2) $\delta = 160.0$ (C^{B3}), 155.2 (C^{A2}), 148.2 (C^{A6}), 139.6 (C^{B1}), 136.8 (C^{A5}), 135.8 (C^{A4}), 135.6 (C^{b1}), 130.73 (C^{B5}), 121.3 (C^{A3}), 120.1 (C^{B6}), 117.0 ($C^{b2/3}$), 114.7 (C^{B4}), 113.9 (C^{B2}), 72.6 (C^{a5}), 71.4 (C^{a3}), 70.2 (C^{a2}), 70.1 (C^{a4}), 68.2 ppm (C^{a1}); IR (solid): $\tilde{\nu} = 3010$w, 2872m, 1724w, 1605m, 1578s, 1460s, 1441m, 1362w, 1298m, 1277m, 1231w, 1202m, 1119m, 1099m, 1059m, 1018w, 933m, 841s, 777s, 744w, 692m, 611m cm^{-1}; EI-MS: m/z 596.3 $[M]^+$ (calcd 596.3); elemental analysis calcd (%) for $C_{36}H_{40}N_2O_6$ C: 72.46, H 6.76, N 4.69; found C 72.26, H 6.66, N 4.49.

$[Ru(bpy)_2(\mathbf{3})][PF_6]_2$: The complex was synthesized by using the same procedure as for $[Ru(bpy)_2(\mathbf{1})][PF_6]_2$ starting with **3** (71.7 mg, 120 μmol) and *cis*-$[Ru(bpy)_2Cl_2]$ (58.8 mg, 121 μmol). Column chromatography (SiO_2, CH_2Cl_2/MeOH 20:1) yielded $[Ru(bpy)_2(\mathbf{3})][PF_6]_2$ (141 mg, 108 μmol, 90%) as an orange solid. M.p. 99–102 °C; ^{1}H NMR (500 MHz, CD_3CN): $\delta = 8.58$ (d, $J = 8.6$ Hz, 2H; H^{A3}), 8.52 (m, 4H; H^{C3+D3}), 8.33 (dd, $J = 2.0$, 8.5 Hz, 2H; H^{A4}), 8.09 (m, 4H; H^{C4+D4}), 7.89 (d, $J = 5.5$ Hz, 2H; H^{C6}), 7.82 (d, $J = 5.6$ Hz, 2H; H^{D6}), 7.81 (d, $J = 1.7$ Hz, 2H; H^{A6}), 7.44 (m, 4H; H^{C5+D5}), 7.35 (t, $J = 8.0$ Hz, 2H; H^{B5}), 7.00 (m, 4H; H^{B4+B6}), 6.93 (s, 2H; H^{B2}), 5.90 (m, 2H; H^{b1}), 5.25 (dd, $J = 3.3$, 17.3 Hz, 2H; H^{b3}), 5.12 (dd, $J = 1.4$, 10.4 Hz, 2H; H^{b2}), 4.07 (dd, $J = 5.3$, 9.7 Hz, 4H; H^{a1}), 3.97 (dd, $J = 1.2$, 4.2 Hz, 4H; H^{a5}), 3.80 (m, 4H; H^{a2}), 3.65 (dd, $J = 3.5$, 5.7 Hz, 4H; $H^{a3/a4}$), 3.57 ppm (dd, $J = 3.5$, 5.6 Hz, 4H; $H^{a3/a4}$); ^{13}C NMR (126 MHz, CD_3CN): $\delta = 160.5$ (C^{B3}), 158.3 (C^{A2}), 158.0 (C^{D2}), 156.5 (C^{C2}), 153.1 (C^{C3+D3}), 150.0 (C^{A6}), 140.6 (C^{A5}), 138.9 ($C^{C4/D4}$), 138.85 ($C^{C4/D4}$), 137.2 (C^{B1}), 136.77 (C^{A4}), 136.3 (C^{b1}), 131.7 (C^{B5}), 128.7 ($C^{C5/D5}$), 128.6 ($C^{C5/D5}$), 125.5 (C^{A3}), 125.3 (2 C^{C5+D5}), 120.5 (C^{B6}), 117.0 ($C^{b2/3}$), 116.95 (C^{B4}), 113.8 (C^{B2}), 72.5 (C^{a5}), 71.45 ($C^{a3/a4}$), 70.4 ($C^{a3/a4}$), 70.2 (C^{a2}), 68.8 ppm (C^{a1}); ^{19}F NMR (376 MHz, CD_3CN): $\delta = -74.1$ ppm (d, $J = 706$ Hz); IR (solid): $\tilde{\nu} = 3077$w, 2934w, 2881w, 1601w, 1595w, 1463m, 1445m, 1422m, 1301w, 1242w, 1206m, 1051w, 1028w, 825s, 762m, 695w cm^{-1}; UV/Vis (MeCN): λ_{max} (ε) = 456 (15900), 316 (46300), 288 nm (79000 mol^{-1} dm^3 cm^{-1}); emission (MeCN, $\lambda_{exc} = 355$ nm): $\lambda_{max} = 642$ nm; ESIMS: m/z 1155.4 $[M-PF_6]^+$ (calcd 1155.3), 505.2 $[M-2PF_6]^{2+}$ (calcd 505.2); elemental analysis calcd (%) for $C_{56}H_{56}F_{12}N_6O_6P_2Ru$: C 51.74, H 4.34, N 6.46; found C 51.78, H 4.25, N 6.24.

5,5′-Bis[3-(1,4,7,10-tetraoxatridec-12-enylphenyl)]-2,2′-bipyridine (4): Ligand **4** was prepared by the same method as **3** starting with 5,5′-bis(3′-hydroxyphenyl)-2,2′-bipyridine (1.11 g, 3.26 mmol), 1-bromo-3,6,9-trioxaundec-11-ene (2.06 g, 8.15 mmol) and Cs_2CO_3 (4.25 g, 13.0 mmol). Ligand **4** was isolated as a colourless solid (2.01 g, 2.93 mmol, 90%). M.p. 57–58 °C; ^{1}H NMR (500 MHz, CD_2Cl_2): $\delta = 8.94$ (d, $J = 1.8$ Hz, 2H; H^{A6}), 8.56 (d, $J = 8.2$ Hz, 2H; H^{A3}), 8.07 (dd, $J = 2.1$, 8.3 Hz, 2H; H^{A4}), 7.43 (t, $J = 7.9$ Hz, 2H; H^{B5}), 7.29 (d, $J = 7.7$ Hz, 2H; H^{B6}), 7.25 (d, $J = 1.9$ Hz,

2H; H^{B2}), 6.99 (dd, $J=2.1$, 8.2 Hz, 2H; H^{B4}), 5.90 (m, 2H; H^{b1}), 5.26 (dd, $J=1.6$, 17.2 Hz, 2H; H^{b3}), 5.15 (dd, $J=1.3$, 10.4 Hz, 2H; H^{b2}), 4.21 (m, 4H; H^{a1}), 3.99 (d, $J=5.6$ Hz, 4H; H^{a7}), 3.87 (m, 4H; H^{a2}), 3.70 (m, 4H; H^{a3}), 3.63 (m, 8H), 3.57 ppm (m, 4H); ^{13}C NMR (126 MHz, CD_2Cl_2): $\delta=$ 160.0 (C^{B3}), 155.2 (C^{A2}), 148.1 (C^{A6}), 139.6 (C^{B1}), 136.7 (C^{A5}), 135.7 (C^{A4}), 135.6 (C^{b1}), 130.7 (C^{B5}), 121.3 (C^{A3}), 120.1 (C^{B6}), 116.9 ($C^{b2/3}$), 114.6 (C^{B2}), 113.9 (C^{B4}), 72.5, 71.3, 71.1 (2C), 70.2, 70.1, 68.2 ppm (C^{a1}); IR (solid): $\tilde{\nu}=$2868m, 1599m, 1582m, 1464s, 1364m, 1300m, 1232w, 1209m, 1126m, 1107m, 1067m, 932m, 633w cm^{-1}; EI-MS: m/z 685.4 $[M]^+$ (calcd 685.4); elemental analysis calcd (%) for $C_{40}H_{48}N_2O_8$: C 70.16, H 7.06, N 4.09; found C 70.03, H 7.06, N 4.00.

[Ru(bpy)$_2$(4)][PF$_6$]$_2$: The complex was synthesized by using the same procedure as for [Ru(bpy)$_2$(**1**)][PF$_6$]$_2$ starting with 5,5′-bis[3-(1,4,7,10-tetraoxatridec-12-enylphenyl)]-2,2′-bipyridine (420 mg, 613 μmol) and *cis*-[Ru(bpy)$_2$Cl$_2$] (300 mg, 619 μmol). After column chromatography (SiO_2, CH_2Cl_2/MeOH 20:1), [Ru(bpy)$_2$(**4**)][PF$_6$]$_2$ was isolated as an orange solid (793 mg, 571 μmol, 93%). M.p. 77–79 °C; ^{1}H NMR (500 MHz, $CDCl_3$): $\delta=$8.50 (d, $J=$8.6 Hz, 2H; H^{A3}), 8.44 (m, 4H; H^{C3+D3}), 8.13 (d, $J=$ 8.3 Hz, 2H; H^{A4}), 7.99 (t, $J=$8.0 Hz, 2H; $H^{C4/D4}$), 7.95 (t, $J=$7.9 Hz, 2H; $H^{C4/D4}$), 7.79 (d, $J=$4.1 Hz, 4H; H^{C6+D6}), 7.65 (s, 2H; H^{A6}), 7.47 (m, 4H; H^{C5+D5}), 7.22 (t, $J=$8.0 Hz, 2H; H^{B5}), 6.83 (m, 6H; $H^{B2+B4+B6}$), 5.84 (m, 2H; H^{b1}), 5.20 (dd, $J=$1.4, 17.2 Hz, 2H; H^{b3}), 5.09 (d, $J=$10.4 Hz, 2H; H^{b2}), 4.05 (m, 4H; H^{a1}), 3.95 (d, $J=$5.6 Hz, 4H; H^{a6}), 3.81 (m, 4H; H^{a2}), 3.69 (m, 4H; $H^{a3/a4}$), 3.64 (m, 8H; $H^{a3/a4+a5}$), 3.56 ppm (m, 4H; H^{a7}); ^{13}C NMR (126 MHz, $CDCl_3$): $\delta=$159.6 (C^{B3}), 156.8 ($C^{C2/D2}$), 156.3 ($C^{C2/D2}$), 155.1 (C^{A2}), 151.7 ($C^{C6/D6}$), 151.4 ($C^{C6/D6}$), 148.1 (C^{A6}), 140.5 (C^{A5}), 138.3 ($C^{C4/D4}$), 138.25 ($C^{C4/D4}$), 136.3 (C^{A4}), 135.7 (C^{B1}), 134.7 (C^{b1}), 130.8 (C^{B5}), 128.6 ($C^{C5/D5}$), 128.3 ($C^{C5/D5}$), 124.6 ($C^{C3/D3}$), 124.5 ($C^{C3/D3}$), 124.3 (C^{A3}), 119.6 (C^{B6}), 117.1 ($C^{b2/3}$), 116.5 (C^{B4}), 112.7 (C^{B2}), 72.1 (C^{a7}), 70.7 ($C^{a3/a4}$), 70.6 ($C^{a3/a4}$), 69.5 (C^{a2}), 69.4 (C^{a6}), 67.6 ppm (C^{a1}); ^{19}F NMR (376 MHz, CD_3CN): $\delta=-74.09$ ppm (d, $J=$706 Hz); IR (solid): $\tilde{\nu}=$3080w, 2864m, 1601m, 1580m, 1464w, 1445w, 1423w, 1369m, 1302m, 1217m, 1095m, 1063m, 945w, 827s, 764m, 731m, 698w cm^{-1}; UV/Vis (MeCN): λ_{max} (ε)= 456 (16200), 318 nm (56900 mol^{-1} dm^3 cm^{-1}); emission (CH_2Cl_2, $\lambda_{exc}=$ 350 nm): $\lambda_{max}=$636 nm; ESIMS: m/z 1243.2 $[M-PF_6]^+$ (calcd 1243.3), 549.1 $[M-2PF_6]^{2+}$ (calcd 549.2); elemental analysis calcd (%) for $C_{60}H_{64}F_{12}N_6O_8P_2Ru$: C 51.91, H 4.65, N 6.05; found C 51.93, H 4.68, N 5.87.

[Fe(2)$_3$][BF$_4$]$_2$: Ligand **2** (735 mg, 1.45 mmol) was dissolved in MeCN (40 mL) and an aqueous solution (40 mL) of $Fe(BF_4)_2{\cdot}6H_2O$ (488 mg, 1.45 mmol) was added. The solution immediately turned red and was heated at reflux for 12 h. A ^{1}H NMR spectrum of the crude product showed ≈10% of unreacted ligand; $Fe(BF_4)_2{\cdot}6H_2O$ (300 mg, 0.89 mmol) was added and the solution was heated at reflux for 3 days. The reaction mixture was filtered over Celite and Al_2O_3. After removal of solvent from the filtrate, [Fe(**2**)$_3$][BF$_4$]$_2$ was isolated as a red solid which was dried in vacuo (848 mg, 483 μmol, 100%). ^{1}H NMR (400 MHz, $CDCl_3$): $\delta=$8.91 (d, $J=$8.3 Hz, 6H; H^{A3}), 8.36 (d, $J=$7.7 Hz, 6H; H^{A4}), 7.54 (s, 6H; H^{A6}), 7.27 (t, $J=$8.0, 6H; H^{B5}), 6.93 (d, $J=$8.4 Hz, 6H; H^{B6}), 6.79 (m, 12H; H^{B2+B4}), 5.90 (m, 6H; H^{b1}), 5.28 (m, 6H; H^{b3}), 5.18 (dd, $J=$1.4, 10.4 Hz, 6H; H^{b2}), 4.03 (m, 24H), 3.74 ppm (m, 12H; $H^{a1+a2+a3}$); ^{13}C NMR (101 MHz, $CDCl_3$); $\delta=$159.8, 157.5, 150.6, 140.5, 137.8, 135.2, 134.4, 131.0, 125.4, 119.2, 117.4, 116.5, 112.8, 72.3, 68.3, 67.7 ppm; ESIMS: m/z 790.8 $[M-2BF_4]^{2+}$ (calcd 790.3); elemental analysis calcd (%) for $C_{96}H_{96}B_2F_8FeN_6O_{12}$: C 65.69, H 5.51, N 4.79; found C 65.37, H 5.54, N 4.72.

Ligand 5: [Fe(**2**)$_3$][BF$_4$]$_2$ (267 mg, 152 μmol) and second-generation Hoyveda–Grubbs catalyst (19.0 mg, 30.4 μmol) were dissolved in CH_2Cl_2 (250 mL). The solution was stirred at room temperature for 40 days. During this time, additional catalyst was added (10 mg after 10 days, and 5 mg after 25 days). The reaction was quenched with ethyl vinyl ether (5 mL) and the solvent was removed in vacuo to yield a red solid. The ^{1}H NMR and ESI mass spectra of the product confirmed that >95% alkene metathesis had been achieved; the compound was used in the next step without purification. The crude product was dissolved in MeCN (100 mL) and an aqueous solution (30 mL) of Na_2H_2EDTA (283 mg, 760 μmol) and Na_2CO_3 (80.5 mg, 760 μmol) was added. The reaction mixture was heated to 50 °C and stirred at that temperature for 1 h. After 30 min, the red colour had disappeared. The solvent volume was reduced and the solution was extracted with CH_2Cl_2 (3×100 mL). The combined organic layers were dried over $MgSO_4$, filtered and the solvent was removed in vacuo to yield a brown oil. The crude product was dissolved in CH_2Cl_2 (50 mL) and EtOH (50 mL) and the reaction mixture was stirred under an atmosphere of H_2 (1 bar) at room temperature for 2 days in the presence of Pd/C (100 mg, 30 mol% Pd). After column chromatography (SiO_2, CH_2Cl_2, NEt_3 (1–3%)) followed by preparative thin-layer chromatography (Al_2O_3, CH_2Cl_2/MeOH (1%), twice; Al_2O_3, CH_2Cl_2/MeOH (0.6%), once), ligand **5** was isolated as a colourless solid (10.5 mg, 7%, ≈80% pure). ^{1}H NMR (400 MHz, CD_2Cl_2): $\delta=$8.85 (m, 4H; H^{A6}), 8.45 (d, $J=$8.3 Hz, 4H; H^{A3}), 7.97 (dd, $J=$2.3, 8.3 Hz, 4H; H^{A4}), 7.38 (t, $J=$ 7.9 Hz, 4H; H^{B5}), 7.22 (m, 8H; H^{B2+B6}), 6.96 (m, 4H; H^{B4}), 4.17 (m, 8H; H^{a1}), 3.78 (m, 8H; $H^{a2/a3}$), 3.57 (m, 8H; $H^{a2/a3}$), 1.68 ppm (m, 8H; H^{a4}); ESIMS: m/z 988.0 $[M+Na]^+$ (calcd 988.1). The ligand was used in the next step without further purification.

[{Ru(bpy)$_2$}$_2$(5)][PF$_6$]$_4$: The complex was prepared by the same procedure as [Ru(bpy)$_2$(**1**)][PF$_6$]$_2$ starting with ligand **5** (10.8 mg, 11.2 μmol) and *cis*-[Ru(bpy)$_2$Cl$_2$] (10.8 mg, 22.4 μmol). Preparative thick-layer chromatography (Al_2O_3, CH_2Cl_2/MeOH 20:1) gave [{Ru(bpy)$_2$}$_2$(**5**)][PF$_6$]$_4$ as an orange solid (12.1 mg, 5.1 μmol, 46%). M.p. 192–196 °C; ^{1}H NMR (600 MHz, CD_3CN): $\delta=$8.48 (m, 8H; H^{C3+D3}), 8.41 (dd, $J=$2.7, 8.5 Hz, 4H; H^{A3}), 8.16 (m, 4H; H^{A4}), 8.01 (m, 8H; H^{C4+D4}), 7.86 (m, 4H; H^{C6}), 7.78 (m, 8H; H^{A6+D6}), 7.39 (m, 8H; H^{C5+D5}), 7.32 (t, $J=$8.1 Hz, 4H; H^{B5}), 6.98 (dd, $J=$2.0, 8.7 Hz, 4H; H^{B4}), 6.91 (m, 8H; H^{B2+B6}), 4.04 (m, 8H; H^{a1}), 3.71 (m, 8H; H^{a2}), 3.48 (m, 8H; H^{a3}), 1.57 ppm (m, 8H; H^{a4}); ^{13}C NMR (151 MHz, CD_3CN): $\delta=$160.0 (C^{B3}), 157.6 (C^{C2}), 157.3 (C^{D2}), 155.7 (C^{A2}), 152.4 (C^{C6+D6}), 149.3 (C^{A6}), 139.9 (C^{A5}), 138.2 (C^{D4}), 136.4 (C^{B1}), 136.0 (C^{A4}), 131.0 (C^{B5}), 128.1 (C^{C5}), 128.0 (C^{D5}), 124.9 (C^{D3}), 124.7 (C^{C3}), 124.6 (C^{A3}), 119.7 (C^{B6}), 116.2 (C^{B4}), 113.7 (C^{B2}), 71.1 (C^{a3}), 69.3 (C^{a2}), 68.2 (C^{a1}), 26.64 ppm (C^{a4}); ^{19}F NMR (376 MHz, CD_3CN): $\delta=$ −74.09 ppm (d, $J=$706 Hz); ESIMS: m/z 1041.3 $[M-2PF_6]^{2+}$ (calcd 1041.2), 646.0 $[M-3PF_6]^{3+}$ (calcd 645.8), 448.2 $[M-4PF_6]^{4+}$ (calcd 448.1); IR (solid): $\tilde{\nu}=$3086w, 2922m, 2853m, 1601m, 1582m, 1464m, 1445m, 1369w, 1301w, 1211m, 1119m, 1055w, 825s, 761m cm^{-1}; UV/Vis (CH_2Cl_2): λ_{max} (ε)=457 (19700), 316 sh (61800), 290 nm (114300 mol^{-1} dm^3 cm^{-1}); emission (CH_2Cl_2, $\lambda_{exc}=$450 nm): $\lambda_{max}=$617 nm; elemental analysis calcd (%) for $C_{100}H_{92}F_{24}N_{12}O_8P_4Ru_2$: C 50.64, H 3.91, N 7.09; found C 50.58, H 4.12, N 7.13.

[Fe(3)$_3$][BF$_4$]$_2$: Ligand **3** (1.84 g, 3.08 mmol) and $Fe(BF_4)_2{\cdot}6H_2O$ (1.04 g, 3.08 mmol) were dissolved in MeCN (300 mL) and the solution was heated at reflux for 3 days. Filtration over Al_2O_3 and removal of the solvent yielded [Fe(**3**)$_3$][BF$_4$]$_2$ as a red oil (1.93 g, 999 μmol, 93%); ^{1}H NMR (500 MHz, CD_3CN): $\delta=$8.66 (d, $J=$8.5 Hz, 6H; H^{A3}), 8.44 (dd, $J=$1.8, 8.5 Hz, 6H; H^{A4}), 7.75 (d, $J=$1.3 Hz, 6H; H^{A6}), 7.33 (t, $J=$8.0 Hz, 6H; H^{B5}), 7.06 (d, $J=$7.7, 6H; H^{B6}), 6.96 (dd, $J=$2.1, 8.3 Hz, 6H; H^{B4}), 6.89 (s, 6H; H^{B2}), 5.86 (m, 6H; H^{b1}), 5.22 (dd, $J=$1.7, 17.3 Hz, 6H; H^{b3}), 5.10 (dd, $J=$1.5, 10.4 Hz, 6H; H^{b2}), 3.95 (m, 24H; H^{a1+a5}), 3.68 (m, 12H; H^{a2}), 3.58 (m, 12H; H^{a3}), 3.53 ppm (m, 12H; H^{a4}); ^{13}C NMR (126 MHz, CD_3CN): $\delta=$160.5 (C^{B3}), 158.8 (C^{A2}), 153.5 (C^{A6}), 140.0 (C^{A5}), 137.7 (C^{A4}), 137.1 (C^{B1}), 136.3 (C^{b1}), 131.7 (C^{B5}), 125.3 (C^{A3}), 120.6 (C^{B6}), 117.2 (C^{B4}), 117.0 ($C^{b2,b3}$), 113.4 (C^{B2}), 72.5 (C^{a5}), 71.4 (C^{a3}), 70.4 (C^{a4}), 70.2 (C^{a2}), 68.7 ppm (C^{a1}); ^{19}F NMR (376 MHz, $CDCl_3$): $\delta=-153.1$ ppm (s); ESIMS: m/z 923.2 $[M-2BF_4]^{2+}$ (calcd 922.9); UV/Vis (MeCN): λ_{max} (ε)= 336 (102700), 544 nm (8960 mol^{-1} dm^3 cm^{-1}); emission (MeCN, $\lambda_{exc}=$ 340 nm): $\lambda_{max}=$406 nm; elemental analysis calcd (%) for $C_{108}H_{120}N_6O_{18}B_2F_8Fe{\cdot}2H_2O$: C 63.10, H 6.08, N 4.09; found C 63.10, H 6.10, N 4.24.

Ligand 6: [Fe(**3**)$_3$][BF$_4$]$_2$ (1.93 g, 955 μmol) and second-generation Hoyveda–Grubbs catalyst (75.0 mg, 120 μmol) were dissolved in CH_2Cl_2 (955 mL). The solution was stirred at room temperature for 30 days. During this time, additional catalyst was added (75 mg after 8 days, and 30 mg after 20 days). The reaction was quenched with ethyl vinyl ether (5 mL) and the solvent was removed in vacuo to give a red solid. ^{1}H NMR and ESIMS confirmed that >95% alkene metathesis had been achieved, and the compound was used further without purification. The crude product was dissolved in a mixture of EtOH (150 mL) and CH_2Cl_2 (150 mL), and Pd/C (500 mg, 25 mol% Pd) was added. The reaction mix-

ture was stirred under an atmosphere of H_2 (1 bar) at room temperature for 12 h. The ^{1}H NMR and ESI mass spectra of the product confirmed complete hydrogenation. The crude product (≈955 μmol) was dissolved in MeCN (200 mL) and an aqueous solution (20 mL) of Na_2H_2EDTA (1.86 g, 5.00 mmol) and Na_2CO_3 (1.06 g, 10.0 mmol) was added. The reaction mixture was stirred at 50 °C for 3 h; the red colour disappeared after 30 min. The organic solvent was removed in vacuo and the aqueous residue was extracted with CH_2Cl_2 (5×50 mL). The combined organic layers were dried over $MgSO_4$, filtered and the solvent removed in vacuo to yield a brown oil (1.65 g). Part of the residue (440 mg) was purified by preparative thin-layer chromatography (Al_2O_3, CH_2Cl_2/MeOH (1.1%), 6 h elution) on eight plates and ligand **6** was isolated as a colourless oil (113 mg, 66.0 mmol, 26%). ^{1}H NMR (500 MHz, CD_2Cl_2): δ = 8.90 (d, J = 1.8, 6H; H^{A6}), 8.50 (d, J = 8.3 Hz, 6H; H^{A3}), 8.01 (dd, J = 2.2, 8.3 Hz, 6H; H^{A4}), 7.39 (t, J = 7.9 Hz, 6H; H^{B5}), 7.24 (d, J = 7.9 Hz, 6H; H^{B6}), 7.22 (d, J = 1.8 Hz, 6H; H^{B2}), 6.96 (dd, J = 2.1, 8.2 Hz, 6H; H^{B4}), 4.17 (m, 12H; H^{a1}), 3.83 (m, 12H; H^{a2}), 3.67 (m, 12H; H^{a3}), 3.57 (m, 12H; H^{a4}), 3.46 (m, 12H; H^{a5}), 1.62 ppm (m, 12H; H^{a6}); ^{13}C NMR (126 MHz, CD_2Cl_2): δ = 160.0 (C^{B3}), 155.2 (C^{A2}), 148.1 (C^{A6}), 139.5 (C^{B1}), 136.6 (C^{A5}), 135.6 (C^{A4}), 130.7 (C^{B5}), 121.3 (C^{A3}), 120.0 (C^{B6}), 114.6 (C^{B4}), 113.9 (C^{B2}), 71.6 (C^{a1}), 71.4 (C^{a2}), 70.7 (C^{a3}), 70.2 (C^{a4}), 68.2 (C^{a5}), 27.0 ppm (C^{a6}); IR (solid): $\tilde{\nu}$ = 2920m, 2862m, 1722w, 1682m, 1597m, 1580m, 1462s, 1439m, 1362w, 1298m, 1281w, 1231w, 1205m, 1103s, 1063m, 1018m, 995s, 937w, 839s, 779s, 744m, 694m, 652w, 604m cm^{-1}; ESIMS: m/z 1734.6 $[M+Na]^+$ (calcd 1734.8); elemental analysis calcd (%) for $C_{102}H_{114}N_6O_{18}\cdot 2H_2O$: C 70.08, H 6.80, N 4.81; found C 70.18, H 6.94, N 4.92.

[{Ru(bpy)$_2$}$_3$(6)][PF$_6$]$_6$: The complex was prepared by the same procedure as $[Ru(bpy)_2(\mathbf{1})][PF_6]_2$ starting with ligand **6** (27.3 mg, 15.9 μmol) and *cis*-$[Ru(bpy)_2Cl_2]$ (23.6 mg, 48.6 μmol) suspended in EtOH (5 mL). The reaction mixture was heated in a microwave reactor at 120 °C for 40 min. An excess of aqueous NH_4PF_6 (≈1 mmol, 50 mL) was added to the orange solution. The orange precipitate that formed was collected by filtration and washed with water (30 mL) and diethyl ether (30 mL). $[\{Ru(bpy)_2\}_3(\mathbf{6})][PF_6]_6$ was isolated as an orange solid (56.2 mg, 14.7 μmol, 92%). Attempts to separate the two diastereoisomers (see text) by chromatography were unsuccessful. M.p. 170–176 °C; ^{1}H NMR (500 MHz, CD_3CN): δ = 8.55 (d, J = 8.6 Hz, 6H; H^{A3}), 8.50 (t, J = 7.5 Hz, 12H; H^{C3+D3}), 8.29 (d, J = 8.5 Hz, 6H; H^{A4}), 8.06 (m, 12H; H^{C4+D4}), 7.88 (d, J = 5.3 Hz, 6H; H^{C6}), 7.81 (d, J = 5.4 Hz, 6H; H^{D6}), 7.79 (d, J = 1.5 Hz, 6H; H^{A6}), 7.43 (m, 12H; H^{C5+D5}), 7.30 (t, J = 7.9 Hz, 6H; H^{B5}), 6.95 (m, 18H; $H^{B2+B4+B6}$), 4.05 (m, 12H; H^{a1}), 3.75 (m, 12H; H^{a2}), 3.59 (m, 12H; $H^{a3/a4}$), 3.52 (m, 12H; $H^{a3/a4}$), 3.37 (m, 12H; H^{a5}), 1.52 ppm (m, 12H; H^{a6}); ^{13}C NMR (126 MHz, CD_3CN): δ = 160.5 (C^{B3}), 158.3 (C^{D2}), 158.0 (C^{C2}), 156.5 (C^{A2}), 153.1 (C^{C6+D6}), 150.0 (C^{A6}), 140.6 (C^{B1}), 139.0 ($C^{C4/D4}$), 138.9 ($C^{C4/D4}$), 137.2 (C^{A5}), 136.8 (C^{A4}), 131.7 (C^{B5}), 128.7 (C^{D5}), 128.65 (C^{C5}), 125.5 ($C^{C3/D3}$), 125.3 ($C^{C3/D3}$), 120.5 ($C^{B4/B6}$), 117.0 ($C^{B4/B6}$), 113.9 (C^{B2}), 71.6 (C^{a5}), 71.5 ($C^{a3/a4}$), 70.9 ($C^{a3/a4}$), 70.2 (C^{a2}), 68.8 (C^{a1}), 27.3 ppm (C^{a6}); IR (solid): $\tilde{\nu}$ = 3061w, 2929m, 2864m, 1738m, 1728m, 1601m, 1582m, 1464m, 1447m, 1369w, 1302w, 1217m, 1099m, 1059w, 827s, 761m cm^{-1}; UV/Vis (CH_2Cl_2): λ_{max} (ε) = 457 (31200), 355 sh (77000), 318 sh (100100), 290 nm (181000 mol^{-1} dm^3 cm^{-1}); emission (CH_2Cl_2, λ_{exc} = 350 nm): λ_{max} = 621 nm; ESIMS: m/z 1765.7 $[M-2PF_6]^{2+}$ (calcd 1766.4), 1128.5 $[M-3PF_6]^{3+}$ (calcd 1129.28), 811.1 $[M-4PF_6]^{4+}$ (calcd 810.7), 619.8 $[M-5PF_6]^{5+}$ (calcd 619.6), 492.4 $[M-6PF_6]^{6+}$ (calcd 492.2); elemental analysis calcd (%) for $C_{162}H_{162}F_{36}N_{18}O_{18}P_6Ru_3$: C 50.91, H 4.27, N 6.60; found C 50.63, H 4.19, N 6.20.

[Ru(bpy)$_2$(7)][PF$_6$]$_2$: Complex $[Ru(bpy)_2(\mathbf{4})][PF_6]_2$ (193 mg, 139 μmol) and second-generation Hoyveda–Grubbs catalyst (6.0 mg, 9.6 μmol) were dissolved in CH_2Cl_2 (14 mL) and stirred at room temperature for 5 days. The ^{1}H NMR and ESI mass spectra of the reaction mixture indicated about 40% conversion of starting material to product. Further catalyst (16 mg) was added to the reaction mixture, which was stirred for a further 7 days. The ^{1}H NMR spectrum of the mixture showed that the reaction was not complete, and further catalyst (8.0 mg) was added. After 5 days of stirring under ambient conditions, the starting material had been consumed. The crude, unsaturated product was passed through a short chromatography column (Al_2O_3, CH_2Cl_2/MeOH 40:1) and the solvent was removed in vacuo. The intermediate product was then hydrogenated with molecular H_2 (1 atm) in a mixture of EtOH (20 mL) and CH_2Cl_2 (20 mL) in the presence of a catalytic amount of Pd/C (30 mg). The solvent was removed in vacuo, and the product re-dissolved in the minimum amount of CH_2Cl_2. $[Ru(bpy)_2(\mathbf{7})][PF_6]_2$ was purified by preparative thick-layer chromatography (SiO_2, CH_2Cl_2/MeOH 25:1) and was isolated as an orange solid (20.2 mg, 14.8 μmol, 10%; see text). ^{1}H NMR (500 MHz, CD_3CN): δ = 8.63 (d, J = 8.1 Hz, 2H; H^{D3}), 8.56 (t, J = 8.0 Hz, 4H; $H^{C3\,A3}$), 8.35 (dd, J = 2.0, 8.5 Hz, 2H; H^{A4}), 8.22 (td, J = 1.2, 7.9 Hz, 2H; H^{D4}), 8.06 (m, 2H; H^{C4}), 7.90 (d, J = 5.0 Hz, 2H; H^{C6}), 7.84 (d, J = 5.5 Hz, 2H; H^{D6}), 7.82 (d, J = 1.8 Hz, 2H; H^{A6}), 7.55 (m, 2H; H^{D5}), 7.42 (t, J = 6.6 Hz, 2H; H^{C5}), 7.38 (t, J = 8.0 Hz, 2H; H^{B5}), 7.27 (d, J = 7.8 Hz, 2H; H^{B6}), 6.96 (dd, J = 2.2, 8.2 Hz, 2H; H^{B4}), 6.72 (m, 2H; H^{B2}), 3.98 (t, J = 6.1 Hz, 4H; H^{a1}), 3.76 (t, J = 6.0 Hz, 4H; H^{a2}), 3.72–3.45 (m, 8H), 3.38 (m, 4H), 2.30 (m, 4H; H^{a7}), 1.58 ppm (m, 4H; H^{a8}); ^{13}C NMR (126 MHz, CD_3CN): δ = 160.8 (C^{B3}), 158.3 ($C^{C2/D2}$), 158.2 ($C^{C2/D2}$), 156.7 (C^{A2}), 153.5 (C^{A6}), 150.3 (C^{C2+D2}), 140.3 (C^{B1}), 140.1 (C^{D4}), 139.2 (C^{C4}), 137.0 (C^{A5}), 136.3 (C^{A4}), 132.1 (C^{B5}), 129.5 (C^{D5}), 129.0 (C^{C5}), 126.0 ($C^{C3/D3\,A3}$), 125.9 ($C^{C3/D3\,A3}$), 125.6 ($C^{C3/D3\,A3}$), 120.9 (C^{B6}), 118.9 (C^{B4}), 113.0 (C^{B2}), 71.9, 71.8, 71.6, 71.2, 70.1 (C^{a2}), 68.7 (C^{a1}), 34.6 (C^{a7}), 27.0 ppm (C^{a8}); ^{19}F NMR (376 MHz, CD_3CN): δ = −74.1 ppm (d, J = 706 Hz); IR (solid): $\tilde{\nu}$ = 2921m, 2892w, 2853m, 1728m, 1717m, 1601m, 1585w, 1464m, 1446m, 1423m, 1372w, 1352w, 1302w, 1275m, 1243m, 1215m, 1121m, 1093m, 1055m, 1032m, 940w, 876w, 829s, 792m, 767s, 740w, 732m, 695m, 690m, 660m cm^{-1}; UV/Vis (CH_2Cl_2): $\lambda(\varepsilon)$ = 457 (14700), 354 sh (39200), 321 sh (45700), 290 nm (86800 mol^{-1} dm^3 cm^{-1}); emission (MeCN, λ_{exc} = 350 nm): λ_{max} = 641 nm; ESIMS: m/z 1217.6 $[M-PF_6]^+$ (calcd 1217.3), 536.2 $[M-2PF_6]^{2+}$ (calcd 536.2). Satisfactory elemental analysis could not be obtained, presumably because of the sodium content (see text).

Crystal structure determination: Data were collected on a Bruker–Nonius Kappa CCD or Stoe IPDS instrument; data reduction, solution and refinement used the programs COLLECT,[34] SIR92,[35] DENZO/SCALEPACK[36] and CRYSTALS,[37] or Stoe IPDS software[38] and SHELXL97.[39] Structures were analysed by using Mercury v.2.2.[40]

*[Fe(**1**)$_3$][PF$_6$]$_2$·3C$_2$H$_4$Cl$_2$*: $C_{78}H_{82}Cl_6F_{12}FeN_6O_6P_2$; M = 1747.95; purple plate; orthorhombic; space group *Pcab*, a = 22.5632(1), b = 25.4589(2), c = 28.8665(2) Å; U = 16581.9(2) Å^3; Z = 8; ρ_{calcd} = 1.400 Mg m^{-3}; $\mu(Mo_{K\alpha})$ = 0.495 mm^{-1}; T = 173(2) K; 113362 reflections collected (19770 unique); merging r = 0.049; refinement of 11198 reflections (1081 parameters) with $I > 2.5\sigma(I)$ converged at final $R1$ = 0.0704 ($R1$ all data = 0.1038), $wR2$ = 0.0813 ($wR2$ all data = 0.0960); goodness of fit (gof) = 1.050.

*[Ru(bpy)$_2$(**1**)][PF$_6$]$_2$·MeCN*: $C_{46}H_{39}F_{12}N_7O_2P_2Ru$; M = 1112.85; red needle; triclinic; space group $P\bar{1}$, a = 12.449(3), b = 13.757(3), c = 14.219(3) Å; α = 76.49(3), β = 74.54(3), γ = 83.29(3)°; U = 2278.2(8) Å^3; Z = 2; ρ_{calcd} = 1.618 Mg m^{-3}; $\mu(Mo_{K\alpha})$ = 0.512 mm^{-1}; T = 173(2) K; 33505 reflections collected (8048 unique); merging r = 0.1257; refinement of 7300 reflections (669 parameters) with $I > 2.0\sigma(I)$ converged at final $R1$ = 0.0572 ($R1$ all data = 0.0629), $wR2$ = 0.1435 ($wR2$ all data = 0.1493); gof = 1.096.

*[{Ru(bpy)}$_2$(**5**)][PF$_6$]$_4$·C$_2$H$_4$Cl$_2$·2.5 EtOAc*: $C_{112}H_{116}F_{24}N_{12}O_{13}P_4Ru_2$; M = 2691.12; red plate; triclinic; space group $P\bar{1}$, a = 114.116(1), b = 20.075(2), c = 23.409(2) Å; α = 77.354(5), β = 73.193(5), γ = 85.179(5)°; U = 6194.7(11) Å^3; Z = 2; ρ_{calcd} = 1.443 Mg m^{-3}; $\mu(Mo_{K\alpha})$ = 0.437 mm^{-1}; T = 173(2) K; 386895 reflections collected (48568 unique); merging r = 0.050; refinement of 18510 reflections (1825 parameters) with $I > 1.9\sigma(I)$ converged at final $R1$ = 0.0679 ($R1$ all data = 0.1455), $wR2$ = 0.0723 ($wR2$ all data = 0.1851); gof = 1.0375.

*[Ru(bpy)$_2$(**7**)][NaRu(bpy)$_2$(**7**)][PF$_6$]$_5$*: $C_{116}H_{124}F_{30}N_{12}NaO_{16}P_5Ru_2$; M = 2892.26; red block; triclinic; space group $P\bar{1}$, a = 15.154(3), b = 17.614(4), c = 26.892(5) Å; α = 86.54(3), β = 82.28(3), γ = 84.31(3)°; U = 7070(3) Å^3; Z = 2; ρ_{calcd} = 1.359 Mg m^{-3}; $\mu(Mo_{K\alpha})$ = 0.372 mm^{-1}; T = 173(2) K; 89634 reflections collected (24992 unique); merging r = 0.0834; refinement of 21321 reflections (1741 parameters) with $I > 2.0\sigma(I)$ converged at final $R1$ = 0.0658 ($R1$ all data = 0.0763), $wR2$ = 0.1683 ($wR2$ all data = 0.1755); gof = 1.054.

CCDC-736161, 736162, 736163 and 736164 contain the supplementary crystallographic data for this paper. These data can be obtained free of charge from The Cambridge Crystallographic Data Centre via www.ccdc.cam.ac.uk/data_request/cif.

Acknowledgements

We thank the University of Basel, the Swiss National Science Foundation, the Swiss Nanoscience Institute and the Stiftung Stipendien-Fonds des Verbandes der Chemischen Industrie e.V. for financial support. We thank Dr. Daniel Häussinger for recording the 600 MHz NMR spectra, and Dr. Tunde Vig for assistance with the AAS measurements.

[1] E. C. Constable, *Coordination Chemistry of Macrocyclic Compounds*, Oxford University Press, Oxford, **1999**.
[2] K. Gloe (Ed.) *Macrocyclic Chemistry Current Trends and Future Perspectives*, Springer, **2005**.
[3] L. F. Lindoy, *The Chemistry of Macrocyclic Ligand Complexes*, Cambridge University Press, Cambridge, **1990**.
[4] G. A. Melson, *Coordination Chemistry of Macrocyclic Compounds*, Plenum, New York **1979**.
[5] H. J. Kim, S. S. Lee, *Inorg. Chem.* **2008**, *47*, 10807–10809.
[6] *Molecular Catenanes, Rotaxanes and Knots: A Journey Through the World of Molecular Topology* (Eds.: J.-P. Sauvage, C. Dietrich-Buchecker), Wiley-VCH, Weinheim, **1999**.
[7] C. Dietrich-Buchecker, B. X. Colasson, J.-P. Sauvage, *Top. Curr. Chem.* **2005**, *249*, 261–284.
[8] C. O. Dietrich-Buchecker, J.-P. Sauvage, *Angew. Chem.* **1989**, *101*, 192–194; *Angew. Chem. Int. Ed. Engl.* **1989**, *28*, 189–192.
[9] E. E. Fenlon, *Eur. J. Org. Chem.* **2008**, 5023–5035.
[10] R. Herges, *Chem. Rev.* **2006**, *106*, 4820–4842.
[11] K. C. Majumdar, H. Rahaman, B. Roy, *Curr. Org. Chem.* **2007**, *11*, 1339–1365.
[12] M. Scholl, T. M. Trnka, J. P. Morgan, R. H. Grubbs, *Tetrahedron Lett.* **1999**, *40*, 2247–2250.
[13] M. Weck, B. Mohr, J. P. Sauvage, R. H. Grubbs, *J. Org. Chem.* **1999**, *64*, 5463–5471.
[14] C. O. Dietrich-Buchecker, P. A. Marnot, J. P. Sauvage, J. P. Kintzinger, P. Maltese, *New J. Chem.* **1984**, *8*, 573–582.
[15] C. O. Dietrich-Buchecker, J. P. Sauvage, J. P. Kintzinger, *Tetrahedron Lett.* **1983**, *24*, 5095–5098.
[16] C. O. Dietrich-Buchecker, J. P. Sauvage, J. M. Kern, *J. Am. Chem. Soc.* **1984**, *106*, 3043–3045.
[17] D. A. Leigh, P. J. Lusby, R. T. McBurney, A. Morelli, A. M. Z. Slawin, A. R. Thomson, D. B. Walker, *J. Am. Chem. Soc.* **2009**, *131*, 3762–3771, and references therein.
[18] K. H. Song, S. O. Kang, J. Ko, *Chem. Eur. J.* **2007**, *13*, 5129–5134.
[19] T. Kawano, M. Nakanishi, T. Kato, I. Ueda, *Chem. Lett.* **2005**, *34*, 350–351.
[20] A. V. Chuchuryukin, P. A. Chase, H. P. Dijkstra, B. M. J. M. Suijkerbuijk, A. M. Mills, A. L. Spek, G. P. M. van Klink, G. van Koten, *Adv. Synth. Catal.* **2005**, *347*, 447–462.
[21] P. Wang, C. N. Moorefield, G. R. Newkome, *Angew. Chem.* **2005**, *117*, 1707–1711; *Angew. Chem. Int. Ed.* **2005**, *44*, 1679–1683.
[22] A.-C. Laemmel, J.-P. Collin, J.-P. Sauvage, G. Accorsi, N. Armaroli, *Eur. J. Inorg. Chem.* **2003**, 467–474.
[23] J. P. Sauvage, M. Ward, *Inorg. Chem.* **1991**, *30*, 3869–3874.
[24] P. Mobian, J. M. Kern, J. P. Sauvage, *Angew. Chem.* **2004**, *116*, 2446–2449; *Angew. Chem. Int. Ed.* **2004**, *43*, 2392–2395.
[25] J. C. Chambron, J.-P. Collin, V. Heitz, D. Jouvenot, J. M. Kern, P. Mobian, D. Pomeranc, J.-P. Sauvage, *Eur. J. Org. Chem.* **2004**, 1627–1638.
[26] V. I. Sokolov, *Uspekhi Khimii* **1973**, *42*, 1037–1059.
[27] E. C. Constable, C. E. Housecroft, B. M. Kariuki, C. B. Smith, *Supramol. Chem.* **2006**, **18**, 305–309.
[28] E. C. Constable, C. E. Housecroft, M. Neuburger, P. Rösel, S. Schaffner, *Dalton Trans.* **2009**, 4918–4927.
[29] J. Lacour, C. Ginglinger, C. Grivet, G. Bernardinelli, *Angew. Chem.* **1997**, *109*, 660–662; *Angew. Chem. Int. Ed. Engl.* **1997**, *36*, 608–610.
[30] F. Favarger, C. Goujon-Ginglinger, D. Monchaud, J. Lacour, *J. Org. Chem.* **2004**, *69*, 8521–8524.
[31] Spartan 04, Wavefunction Inc.
[32] P. van der Sluis, A. L. Spek, *Acta Crystallogr. Sect. A* **1990**, *46*, 194–201.
[33] G. Sprintschnik, H. W. Sprintschnik, P. P. Kirsch, D. G. Whitten, *J. Am. Chem. Soc.* **1977**, *99*, 4947–4954.
[34] COLLECT Software, Nonius BV **1997–2001**.
[35] A. Altomare, G. Cascarano, G. Giacovazzo, A. Guagliardi, M. C. Burla, G. Polidori, M. Camalli, *J. Appl. Crystallogr.* **1994**, *27*, 435–435.
[36] Z. Otwinowski, W. Minor, *Methods in Enzymology, Vol. 276* (Eds.: C. W. Carter, Jr., R. M. Sweet), Academic Press, New York, **1997**, p. 307.
[37] P. W. Betteridge, J. R. Carruthers, R. I. Cooper, K. Prout, D. J. Watkin, *J. Appl. Crystallogr.* **2003**, *36*, 1487–1487.
[38] Stoe & Cie, IPDS software v. 1.26, Stoe & Cie, Darmstadt, **1996**.
[39] G. M. Sheldrick, *Acta Crystallogr. Sect. A* **2008**, *64*, 112–122.
[40] I. J. Bruno, J. C. Cole, P. R. Edgington, M. K. Kessler, C. F. Macrae, P. McCabe, J. Pearson, R. Taylor, *Acta Crystallogr. Sect. B* **2002**, *58*, 389–397.

Received: June 16, 2009
Published online: September 16, 2009

